

NCHRP Report 350 Evaluation of the Nebraska Thrie-Beam Transition

SPR-PL-1(34) P500



by

Brian G. Pfeifer, Ph.D., P.E.
Research Associate Engineer

Ronald K. Faller, Ph.D., P.E.
Research Associate Engineer

John D. Reid, Ph.D.
Assistant Professor

Midwest Roadside Safety Facility

University of Nebraska-Lincoln
W328.1 Nebraska Hall
Lincoln, Nebraska 68588-0529
(402) 472-9198

Submitted to

Nebraska Department of Roads

1500 Nebraska Highway 2
Lincoln, Nebraska 68502

Research Report No. TRP-03-70-98

May 1998

Technical Report Documentation Page

1. Report No. SPR-PL-1(34) P500		2.		3. Recipient's Accession No.	
4. Title and Subtitle NCHRP Report 350 Evaluation of the Nebraska Thrie-Beam Transition		5. Report Date May 1998		6.	
		7. Author(s) Brian G. Pfeifer, Ronald K. Faller, and John D. Reid		8. Performing Organization Report No. TRP-03-70-98	
9. Performing Organization Name and Address Midwest Roadside Safety Facility (MwRSF) University of Nebraska - Lincoln W328.1 Nebraska Hall Lincoln, NE 68588-0529		10. Project/Task/Work Unit No.		11. Contract © or Grant (G) No. SPR-PL-1(34) P500	
		12. Sponsoring Organization Name and Address Nebraska Department of Roads 1500 Nebraska Highway 2 Lincoln, Nebraska 68502		13. Type of Report and Period Covered Final Report 1998	
15. Supplementary Notes Prepared in cooperation with the U.S. Department of Transportation, Federal Highway Administration.					
16. Abstract (Limit: 200 words) <p>This project was initiated to develop a thrie-beam transition to a concrete bridge rail which is capable of passing the criteria set forth in NCHRP Report 350. The system currently used by the Nebraska Department of Roads was redesigned with the help of the BARRIER VII computer program. This redesigned system was subjected to one test with a 2000-kg pickup impacting the system at 100 km/h and 25 degrees. The vehicle was redirected in a stable and controlled manner, but considerable occupant compartment damage occurred during the impact, resulting in failure of the test.</p>					
17. Document Analysis/Descriptors Highway Safety, Guardrail, Longitudinal Barrier, Approach Guardrail,			18. Availability Statement No restrictions. Document available from: National Technical Information Services, Springfield, Virginia 22161		
19. Security Class (this report) Unclassified		20. Security Class (this page) Unclassified		21. No. of Pages 56	22. Price

DISCLAIMER STATEMENT

The contents of this report reflect the views of the authors who are responsible for the facts and the accuracy of the data presented herein. The contents do not necessarily reflect the official views or policies of the Nebraska Department of Roads nor the Federal Highway Administration. This report does not constitute a standard, specification, or regulation.

ACKNOWLEDGEMENTS

The authors wish to acknowledge the Nebraska Department of Roads for funding the research described herein. A special thanks is given to the following individuals who made a contribution to the completion of this research project.

Nebraska Department of Roads

Leona Kolbet, Research Coordinator
Phil Tenhulzen, Design Standards Engineer
Mark Osborn, Engineer
Bruce Thill, Policy and Standards Engineer
Mark Burnham, Physical Test Engineer
Stan Karel, Engineering Unit Supervisor

Federal Highway Administration

Milo Cress, P.E., Nebraska Division Office

Midwest Roadside Safety Facility

Dean L. Sicking, Ph.D., P.E., Director
John R. Rohde, Ph.D., P.E., Associate Professor
James C. Holloway, Research Associate Engineer
Kenneth L. Krenk, Field Operations Manager
Michael L. Hanau, Laboratory Mechanic I
Eric A. Keller, Computer Technician II
Undergraduate and Graduate Assistants

Dunlap Photography

James Dunlap, Owner

TABLE OF CONTENTS

	Page
DISCLAIMER STATEMENT	i
ACKNOWLEDGEMENTS	ii
LIST OF FIGURES	v
LIST OF TABLES	vi
1 INTRODUCTION	1
1.1 Objective	2
1.2 Scope	2
2 DESIGN DETAILS	3
3 COMPUTER SIMULATION	8
3.1 Introduction	8
3.2 Design Alternatives	9
3.3 Results	9
4 TEST CONDITIONS	11
4.1 Test Facility	11
4.1.1 <u>Test Site</u>	11
4.1.2 <u>Vehicle Guidance System</u>	11
4.2 Test Vehicle	11
4.3 Data Acquisition Systems	14
4.3.1 <u>Accelerometers</u>	14
4.3.2 <u>High Speed Photography</u>	14
4.3.3 <u>Speed Trap Switches</u>	15
4.3.4 <u>Strain Gauges</u>	15
5 PERFORMANCE EVALUATION CRITERIA	17
6 TEST RESULTS	19
6.1 Test NEBT-1 (2000P, 100 km/h, 25 degrees)	19
7 STRAIN GAUGE RESULTS	30
8 DISCUSSION	31

9 RECOMMENDATIONS	33
10 CONCLUSIONS	34
11 REFERENCES	35
12 APPENDICES	36
APPENDIX A: Nebraska Transition Design Details	37
APPENDIX B: BARRIER VII Simulation Input	49
APPENDIX C: Accelerometer Data Analysis - Test NEBT-1	52

LIST OF FIGURES

	Page
Figure 1. Original Nebraska Transition Design	5
Figure 2. Redesigned Nebraska Transition	7
Figure 3. Test Vehicle, Test NEBT-1	12
Figure 4. Test Vehicle Dimensions, Test NEBT-1	13
Figure 5. Summary of Test NEBT-1.	22
Figure 6. Downstream Sequential Photographs, Test NEBT-1.	23
Figure 7. Close-up Sequential Photographs, Test NEBT-1.	24
Figure 8. Vehicle Trajectory, Test NEBT-1.	25
Figure 9. System Damage, Test NEBT-1.	26
Figure 10. Vehicle Damage, Test NEBT-1.	28

LIST OF TABLES

	Page
Table 1. Relevant NCHRP 350 Evaluation Criteria	18
Table 2. Strain Gauge Instrumentation Results	30

1 INTRODUCTION

Guardrails are intended to protect the traveling public from hazardous obstacles, both natural and man made, which are located within the clearzone of a roadway. These are usually flexible systems which are designed to deflect during the redirection of an impacting vehicle. Bridge rails serve a similar purpose, as they prevent errant vehicles from proceeding over the edge of a bridge, and in the case of overpasses, they protect the traffic and pedestrians below the bridge as well. Bridge rails are normally much more rigid than guardrails, as there is little room for deflection on the edge of a bridge. The difference in stiffness between these systems leads to a potentially dangerous situation when an approach guardrail is transitioned to a rigid bridge rail.

If the approach guardrail is too flexible, vehicles impacting in this transition area will “pocket” and impact the end of the bridge rail. This type of accident results in very high deceleration rates and considerable deformation of the occupant compartment, as well as very serious injury or death to the occupants. In order to avoid this behavior, it is necessary to gradually stiffen the approach guardrail so that large deflections do not occur near the end of the bridge rail.

There has been a significant amount of research conducted in this area, with the majority of the work being concentrated on designing systems which meet the performance requirements of NCHRP Report 230 (1). This criteria has been in effect since 1981, and requires that the system pass a full-scale vehicle crash test consisting of a 4500-lb sedan impacting at 60 mph and 25 degrees. The impact location for this test is specified to be 15 ft upstream of the bridge rail end. A large number of guardrail to bridge rail transitions have been tested and approved under this criteria, and have been installed throughout the country. In 1993, a new set of criteria was introduced to the highway safety community in NCHRP Report

350 (2). This criteria reflected the recent increase in the popularity of light trucks and sport utility vehicles by replacing the 4500-lb sedan, previously used as a test vehicle, with a ¾-ton pickup truck. The impact conditions for this test are similar, 100 km/hr (62.2 mph) and 25 degrees, but the impact point is now determined based on the predicted worst case for the system. This is referred to as the critical impact point (CIP) and is described later in this report in more detail.

The introduction of the ¾-ton pickup as a test vehicle has presented a number of challenges to designers of roadside appurtenances. The higher center of gravity and bumper height of this vehicle results in a less stable impact response, often resulting in the vehicle ramping over the system or rolling over after the initial impact. The structural design of the pickup is such that significantly more occupant compartment deformation is present after a redirection test, as compared to a similar test with a full-size sedan.

1.1 Objective

The objective of this research project was to redesign the guardrail to bridge rail transition used by the Nebraska Department of Roads so that it is capable of passing the criteria required by NCHRP Report 350 (2).

1.2 Scope

The scope of this project included the analysis and simulation of the current guardrail to bridge rail transition, and the subsequent redesign of the system to meet the criteria set forth in NCHRP Report 350 (2). The redesigned system was then evaluated with a full-scale vehicle crash test consisting of a 2000-kg pickup impacting the transition at 100 km/h and 25 degrees.

2 DESIGN DETAILS

The design details of the original Nebraska Thrie-Beam Transition, which was successfully tested to NCHRP Report 230 criteria in 1987 (3), is shown in Figure 1. This design has been very popular because it allows what would normally be the first post in the transition (with 3 ft - 1½ in. spacing) to be omitted from the system. This is often necessary due to obstructions caused by the bridge substructure being located in this area. The obvious problem with this type of design is that the missing post allows additional deflection at a critical point and introduces the possibility of snagging on the end of the bridge rail. This problem is countered by nesting the thrie-beam in this area and incorporating a flare into the end of the concrete parapet to reduce the potential for snagging. The size of the posts in the transition area are also increased, in an effort to minimize the deflection during an impact.

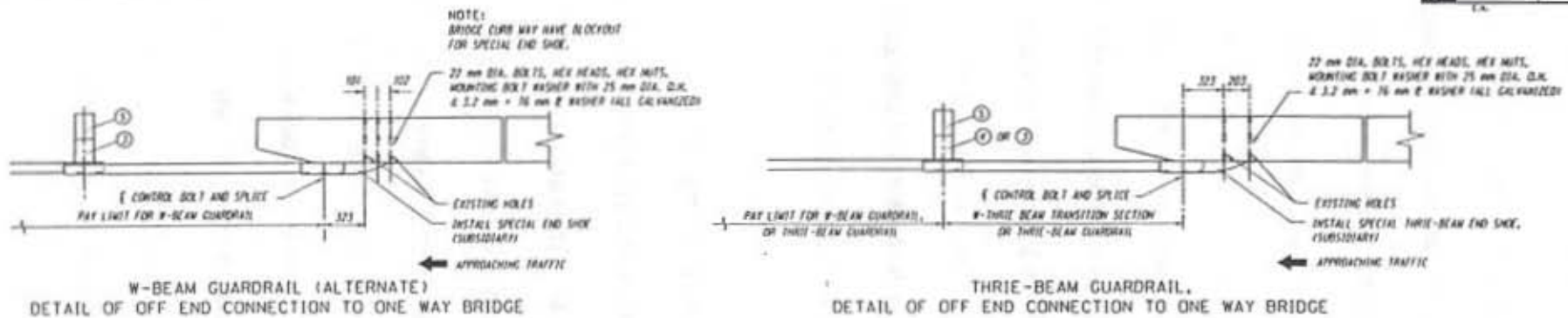
Although this design was capable of passing the NCHRP Report 230 testing with the full-size sedan, a new array of variables is introduced with the pickup testing required by NCHRP Report 350, as discussed in the introduction. The most critical of these differences being the higher center of gravity and the difference in vehicle structure which typically allows more occupant compartment deformation for a given redirection impact. With these design challenges in mind, the transition system was redesigned with the goal of producing a system which could pass the criteria required by NCHRP Report 350. The details of the BARRIER VII (4) computer modeling effort, which was key to the redesign procedure, are presented in the next section.

The redesigned system is shown in Figure 2, with detailed component drawings presented in Appendix A. Several design changes were introduced, including the modification of the concrete abutment so that the flared portion continues down to the bridge deck surface. This was done to improve

constructability and reduce the likelihood of the vehicle snagging on the end of the bridge rail. Other modifications were also made to the geometry of this abutment to reduce vehicle snag, as shown in the design drawings. These changes were based on BARRIER VII simulations which considered the amount of wheel hub snag which would occur as a result of contact with the abutments.

First, the flare rate of the tapered end was increased in order to move the concrete end further behind the back face of the three beam rail. This resulted in the concrete end being positioned 175 mm (6.9 in.) behind the rail in the modified design versus 115 mm (4.5 in.) in the original design. Second, the length of the tapered section was decreased from 460 mm (18.1 in.) to 250 mm (9.8 in.) to reduce the required distance the concrete end needed to be offset from the back of the three beam rail as well as to reduce construction costs. The increased flare rate and decreased length of the flared portion of the abutment are the result of the BARRIER VII analysis.

The Nebraska Department of Roads has recently begun to use steel posts in guardrail systems instead of wood posts. As a result of this change, it was requested that the redesigned system utilize steel posts. This also made the design more reasonable, as the strength of the steel post could be increased without an unreasonably large increase in post size, as would have been necessary with a wood post. As can be seen in Figure 2, a 102-mm (4-in.) concrete slab was poured around the first five posts in the transition, with a 330-mm by 400-mm (13-in. by 15³/₄-in.) recess around each post. A 51-mm (2-in.) thick layer of flowable fill was then poured around each post for vegetation control. This is a weak mix (specifications presented in Appendix A), which should not significantly affect the performance of the post.



**CONNECTION NOTES:
FOR DIVIDED ROADWAY**

- INSTALL SPECIAL THREE-BEAM END SHOE BETWEEN NESTED GUARDRAIL ELEMENTS (SUBSIDIARY TO BRIDGE APPROACH SECTION)

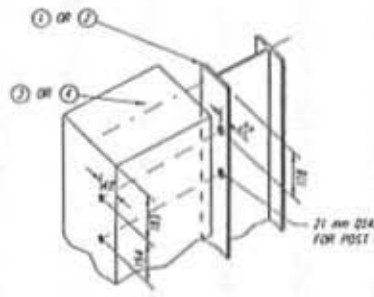
FOR 2-LANE ROADWAY

FOR APPROACHING TRAFFIC

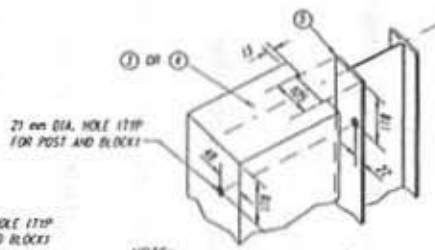
- INSTALL SPECIAL THREE-BEAM END SHOE BETWEEN NESTED GUARDRAIL ELEMENTS.

FOR OFF END CONNECTIONS

- INSTALL SPECIAL THREE-BEAM END SHOE OUTSIDE OF THE NESTED GUARDRAIL ELEMENTS.



**STEEL POST WITH WOOD OFFSET BLOCK
ALTERNATE**

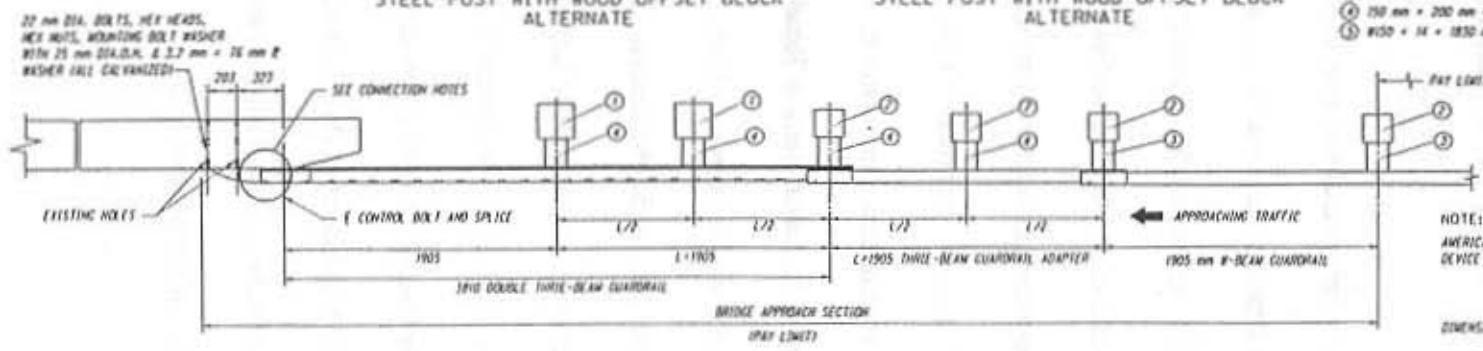


**STEEL POST WITH WOOD OFFSET BLOCK
ALTERNATE**

NOTE:
IF A 60 NAIL IS USED TO PREVENT BLOCK FROM ROTATION, NO ROUTING IS NECESSARY.

- LEGEND (FOR WOOD POSTS)**
- ① 250 mm x 250 mm x 1830 SAVED TREATED TIMBER POST
 - ② 200 mm x 200 mm x 1830 SAVED TREATED TIMBER POST
 - ③ 150 mm x 200 mm x 360 SAVED TREATED TIMBER OFFSET BLOCK
 - ④ 150 mm x 200 mm x 554 SAVED TREATED TIMBER OFFSET BLOCK
 - ⑤ 150 mm x 200 mm x 1830 SAVED TREATED TIMBER POST

- LEGEND (FOR STEEL POSTS)**
- ① W50 x 37 x 1830 mm OH WOOD x 31 x 1830 mm POST
 - ② W50 x 30 x 1830 mm OH WOOD x 27 x 1830 mm POST
 - ③ 150 mm x 200 mm x 256 mm SAVED TREATED TIMBER OFFSET BLOCK
 - ④ 150 mm x 200 mm x 560 mm SAVED TREATED TIMBER OFFSET BLOCK
 - ⑤ W50 x 14 x 1830 mm POST



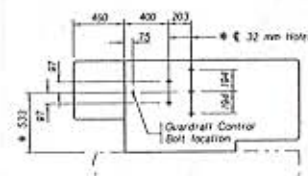
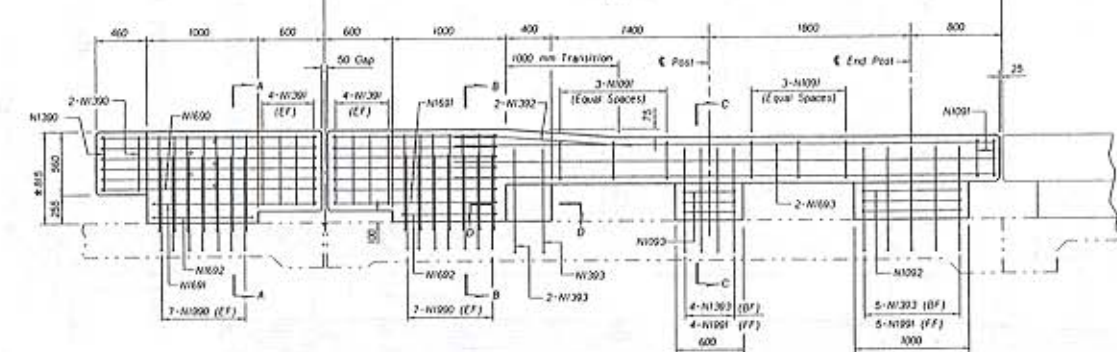
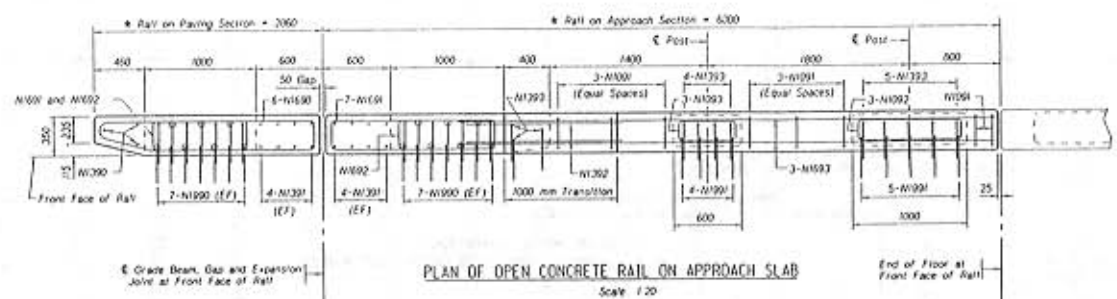
NOTE:
AMERICAN STANDARD HARDWARE WILL BE USED UNTIL THIS DEVICE HAS BEEN CRASHED TESTED USING METRIC FASTENERS.

DIMENSIONS ARE IN MILLIMETERS UNLESS OTHERWISE SHOWN.

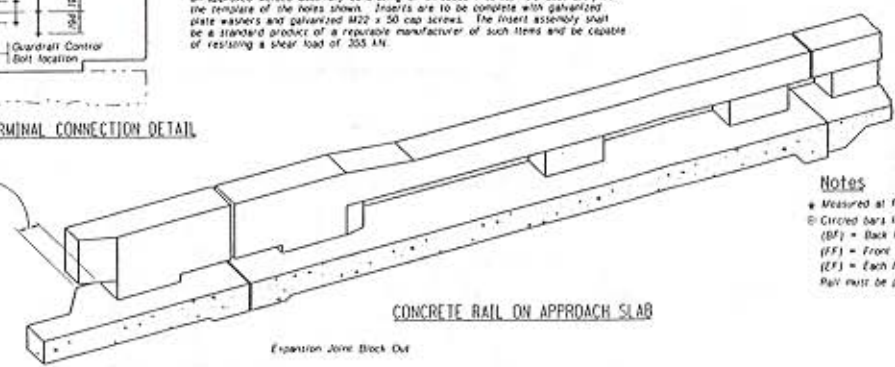
DETAILS OF BRIDGE APPROACH SECTION

**BRIDGE APPROACH SECTION
SHEET OF
SPECIAL PLAN C**

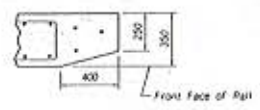
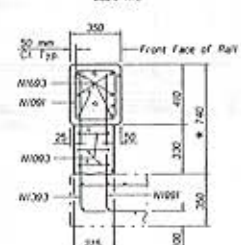
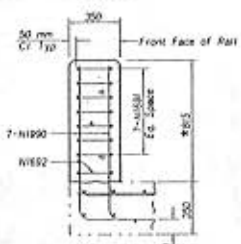
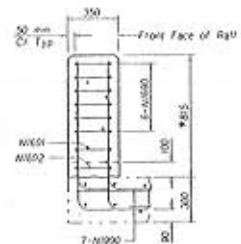
Figure 1. Original Nebraska Transition Design.



As an alternate method, the contractor shall furnish and cast into the concrete an approved welded assembly consisting of threaded inserts, held accurately to the template of the holes shown. Inserts are to be complete with galvanized plate washers and galvanized M22 x 50 cap screws. The insert assembly shall be a standard product of a reputable manufacturer of such items and be capable of resisting a shear load of 255 kN.



- Notes**
- Measured at Front Face of rail.
 - Circled bars indicate placement in the top layer.
 - (BF) = Back Face
 - (FF) = Front Face
 - (EF) = Each Face
 - Rail must be plumb.



ALL STATIONS AND ELEVATIONS ARE METERS [m]. ALL DIMENSIONS ARE MILLIMETERS [mm] UNLESS OTHERWISE NOTED.

Figure 1. Original Nebraska Transition Design (continued).

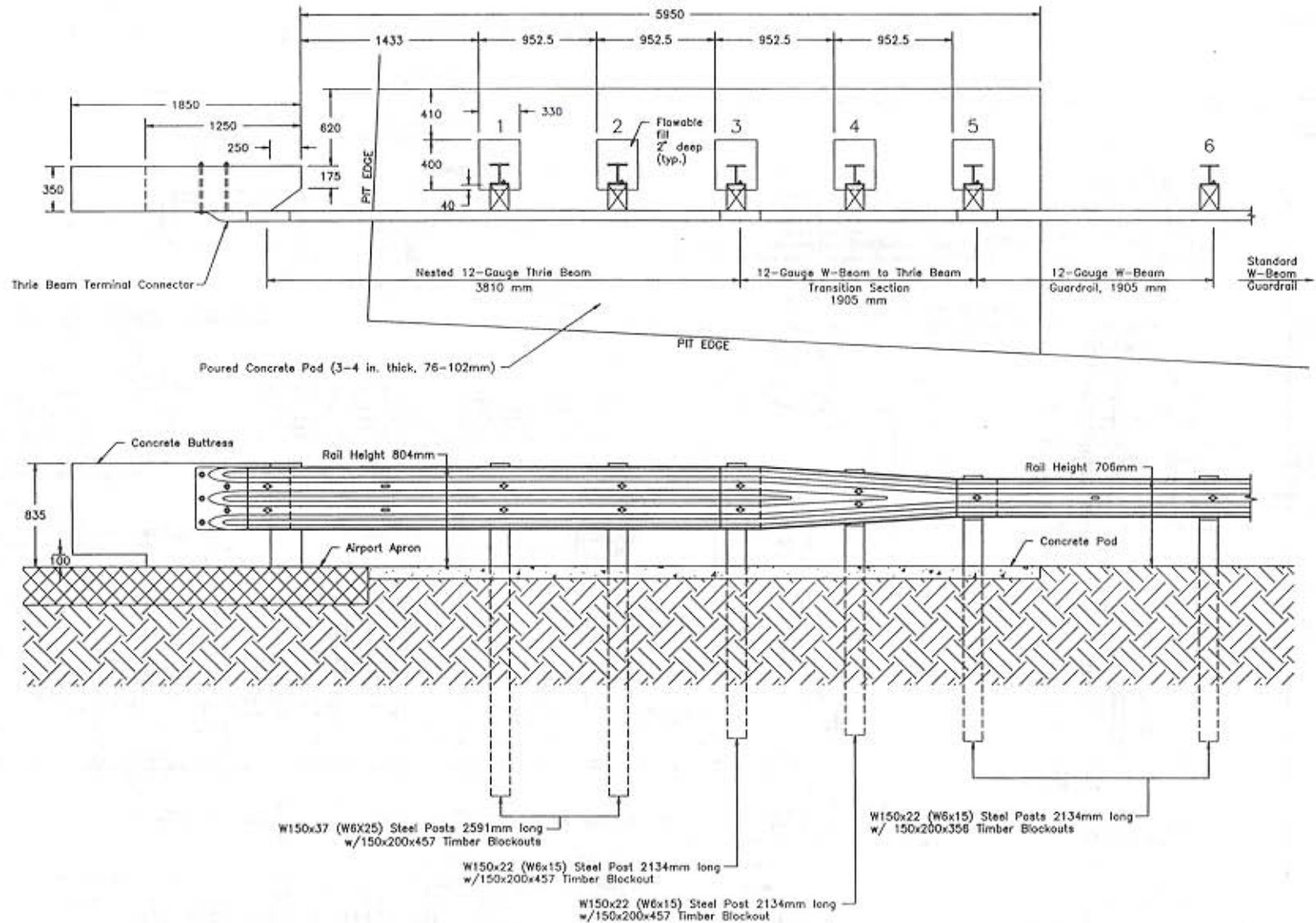


Figure 2. Redesigned Nebraska Transition.

3 COMPUTER SIMULATION

3.1 Introduction

Prior to full-scale vehicle crash testing, the BARRIER VII (4) computer model was used to analyze and predict the dynamic performance of various approach guardrail transition alternatives attached to Nebraska's standardized concrete buttress. The simulations were modeled with a 2000-kg pickup truck impacting at a speed of 100.0 km/hr and at an angle of 25 degrees. A typical computer simulation input data file is shown in Appendix B.

Computer simulation was also used to determine the critical impact point (CIP) for the approach guardrail transition. The CIP was based upon the impact condition which produced the greatest potential for wheel-assembly snagging on the lower blunt-end face on the upstream end of the concrete buttress, occurring in combination with the maximum lateral dynamic rail deflection. Generally, it is believed that wheel snag distances, in excess of 51 mm (2 in.) for the steel rim, results in an increased potential for snagging and contact on the blunt-end face of the concrete barrier. In this design, however, the researchers modified the size and shape of the taper on the upstream end of the concrete buttress in an attempt to completely eliminate all wheel and rim contact. The size of the redesigned taper was 250-mm (9.8-in.) long and 175-mm (6.9-in.) wide, while the original taper was 460-mm (18.1-in.) long by 115-mm (4.5-mm) wide.

Past research involving sedan crash tests into transitions has shown that the potential for vehicle pocketing is significantly reduced when the maximum dynamic rail deflections are less than 305 mm (12 in.). However, recent pickup truck crash tests conducted according to NCHRP 350 on three beam transitions have shown that the maximum allowable dynamic rail deflection should be less than this limit due to the

increased propensity for vehicle rollover. Currently, it is believed that a maximum dynamic rail deflection of between 203 to 229 mm (8 to 9 in.), as measured to the top of the rail, should be allowed for TL-3 three beam transitions.

3.2 Design Alternatives

The new approach guardrail transition was designed with consideration for eliminating wheel snag on the concrete buttress and not allowing dynamic rail deflections greater than 203 to 229 mm (8 to 9 in.), as measured to the top of the rail. Two steel post alternatives were configured to meet these design considerations. The first alternative (Option No. 1) was supported by two W150x37 (W6x25) by 2591-mm (8½-ft) long steel posts and four W150x22 (W6x15) by 2134-mm (7-ft) long steel posts. Post spacings consisted of one at 1879 mm (6 ft - 2 in.), four at 953 mm (3 ft - 1½ in.), and one at 1905 mm (6 ft - 3 in.). The second alternative (Option No. 2) was supported by four W200x46 (W8x31) by 3048-mm (10-ft) long steel posts and three W150x22 (W6x15) by 2134-mm (7-ft) long steel posts. Post spacings consisted of one at 1879 mm (6 ft - 2 in.), two at 476 mm (1 ft - 6¾ in.), three at 953 mm (3 ft - 1½ in.), and one at 1905 mm (6 ft - 3 in.).

3.3 Results

For Option No. 1 (W150x37), the critical impact point was determined to be the midspan between post nos. 1 and 2 or 2105 mm (7 ft - 1 in.) from the upstream end of the concrete end section. For this impact condition, wheel snag distances for the outer tire and inner steel rim were calculated to be approximately 9.5 mm (¾ in.) and 0 mm, respectively. For this impact location, the predicted maximum lateral dynamic rail deflection was 203 mm (8 in.), as measured to the center height of the rail. Subsequently, the maximum dynamic rail deflection at the top of the rail was estimated to be 234 mm (9.2

in.).

For Option No. 2 (W200x46), the critical impact point was determined to be post no. 2 or 2105 mm (7 ft - 1 in.) from the upstream end of the concrete end section. For this impact condition, it was predicted that wheel snag would not occur on either the outer tire and inner steel rim. For this impact location, the predicted maximum lateral dynamic rail deflection was 184 mm (7¼ in.), as measured to the center height of the rail. Subsequently, the maximum dynamic rail deflection at the top of the rail was estimated to be 208 mm (8.2 in.).

A comparison of the two options revealed that for both systems, wheel snag distances were found to be negligible and the maximum dynamic rail deflections to the top of rail were within the design limits. Therefore, Option 1 (W150x37) was selected over Option 2 (W200x46), since the significant increase in construction costs for Option 2 over Option 1 provided only a slight reduction in wheel snag distances and dynamic rail deflections.

4 TEST CONDITIONS

4.1 Test Facility

4.1.1 Test Site

The Midwest Roadside Safety Facility's outdoor test site is located at the Lincoln Air-Park on the northwest end of the Lincoln Municipal Airport. The test facility is approximately 8 km (5 miles) northwest of the University of Nebraska-Lincoln. The site is surrounded and protected by a 2.4 m (8-ft) high chain-link security fence.

4.1.2 Vehicle Guidance System

A reverse cable tow system with a 1:2 mechanical advantage was used to propel the test vehicle. The distance traveled and the speed of the tow vehicle are one-half that of the test vehicle. The test vehicle was released from the tow cable before impact with the appurtenance. A fifth wheel, built by the Nucleus Corporation, was used in conjunction with a digital speedometer to increase the accuracy of the test vehicle impact speed.

A vehicle guidance system developed by Hinch (5) was used to steer the test vehicle. The guide-flag, attached to the front-left wheel and the guide cable, was sheared off before impact. The 95-mm (3/8-in.) diameter guide cable was tensioned to approximately 13.3 kN (3,000 lbs), and supported laterally and vertically every 30.5 m (100 ft) by hinged stanchions. The vehicle guidance system was 460-m (1,500-ft) long for the test.

4.2 Test Vehicle

The test vehicle used for this evaluation was a 1990 ¾-ton Chevrolet pickup with a test inertial mass of 2000 kg (4410 lbs). Photographs of this vehicle are shown in Figure 3, with dimensions being presented in Figure 4.

A number of square, black and white-checked targets were placed on the test vehicle for use in the high-speed film analysis. Two targets were located on the center of gravity, one on the top and one on the driver's side of the test vehicle. The remaining targets were strategically located so they could be used in the film analysis of the test.

The front wheels of the test vehicle were aligned for camber, caster, and toe-in values of zero so that the vehicle would track properly along the guide cable. Two 5B flash bulbs were mounted on the roof of the vehicle to pinpoint the time of impact with the guardrail on the high-speed film. The flash bulbs were fired by a pressure tape switch mounted on the front face of the bumper.

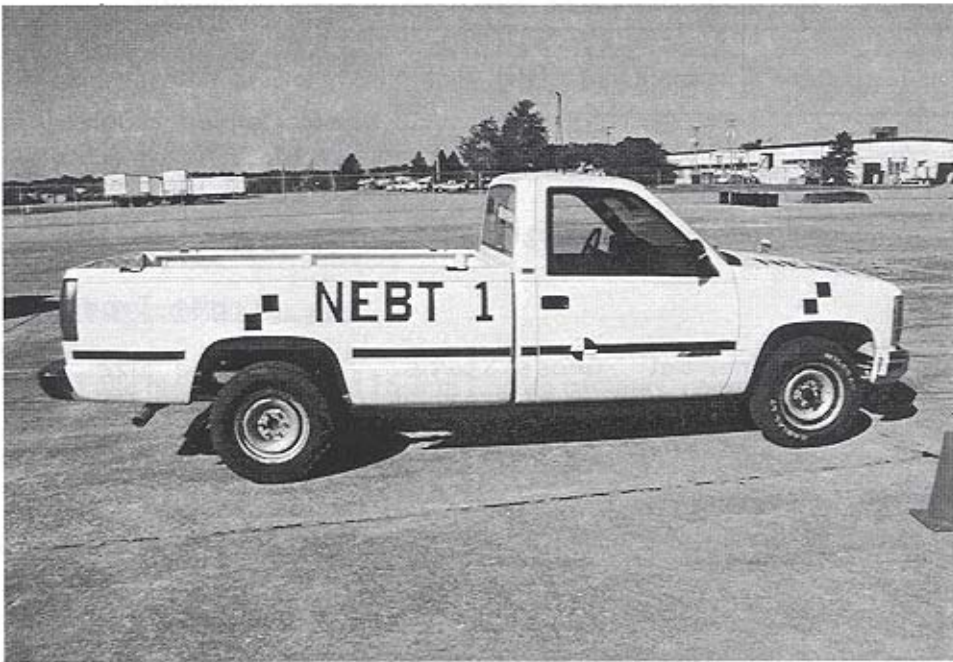
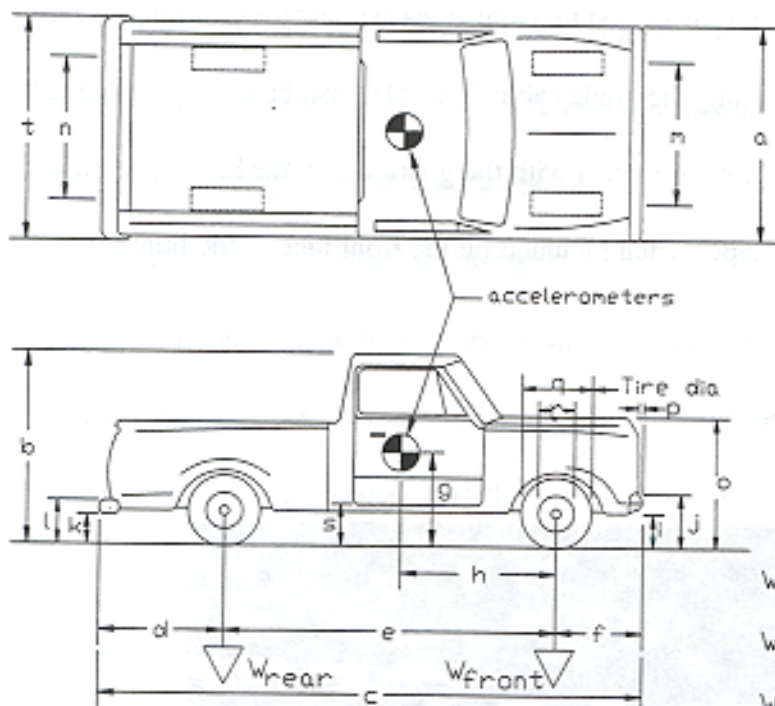


Figure 3. Test Vehicle, Test NEBT-1.

Date: 10-2-97 Test Number: NEBT-1 Model: 2500
 Make: Chevrolet Vehicle I.D.#: 1GCFC24KXLE189207
 Tire Size: 225/75 R16 Year: 1990 Odometer: 064550

*(All Measurements Refer to Impacting Side)



Vehicle Geometry - mm

a 1867 b 1803
 c 5510 d 1295
 e 3340 f 875
 g 711 h 1500
 i 432 j 635
 k 560 l 745
 m 1588 n 1613
 o 1003 p 83
 q 750 r 445
 s 406 t 1842

Wheel Center Height Front 350
 Wheel Center Height Rear 356
 Wheel Well Clearance (FR) 845
 Wheel Well Clearance (RR) 908

Weights - kg	Curb	Test Inertial	Gross Static
W_{front}	<u>1033</u>	<u>1103</u>	<u>1103</u>
W_{rear}	<u>839</u>	<u>901</u>	<u>901</u>
W_{total}	<u>1872</u>	<u>2004</u>	<u>2004</u>

Engine Type V-8
 Engine Size 5.7 L
 Transmission Type:
 Automatic or Manual
 FWD or RWD or 4WD

Note any damage prior to test: None

Figure 4. Test Vehicle Dimensions, Test NEBT-1.

4.3 Data Acquisition Systems

4.3.1 Accelerometers

One triaxial piezoresistive accelerometer system, with a range of ± 200 G's, was used to measure the acceleration in the longitudinal, lateral, and vertical directions, at a sample rate of 10,000 Hz. The environmental shock and vibration sensor/recorder system, Model EDR-4M6, was developed by Instrumented Sensor Technology (IST) of Okemos, Michigan and includes three differential channels as well as three single-ended channels. The EDR-4 was configured with 6 Mb of RAM memory and a 1,500 Hz lowpass filter. Computer software, "DynaMax 1 (DM-1)" and "DADiSP" were used to digitize, analyze, and plot the accelerometer data.

A backup triaxial piezoresistive accelerometer system, with a range of ± 200 G's, was also used to measure the acceleration in the longitudinal, lateral, and vertical directions, at a sample rate of 3,200 Hz. The environmental shock and vibration sensor/recorder system, Model EDR-3, was developed by Instrumented Sensor Technology (IST) of Okemos, Michigan. The EDR-3 was configured with 256 Kb of RAM memory and a 1,120 Hz lowpass filter. Computer software, "DynaMax 1 (DM-1)" and "DADiSP" were used to digitize, analyze, and plot the accelerometer data .

4.3.2 High Speed Photography

Five Red Lake brand high-speed 16-mm Locam cameras, operating at 500 frames/sec, were used to film the crash test. One camera, with a 12.5-mm lens, was placed above the test installation to provide a field of view perpendicular to the ground. A second Locam, with a 17 to 102 mm zoom lens, was placed downstream from the impact point and had a field of view parallel to the barrier. A third Locam, with a 12.5 to 75-mm zoom lens, was placed on the traffic side of the bridge rail and had a field of view perpendicular to the barrier. Two additional high speed Locam cameras were placed behind the rail to aid

in evaluation of the vehicle/rail interaction.

The film was analyzed using a Vanguard Motion Analyzer. Actual camera speed and camera divergence factors were considered in the analysis of the high-speed film.

4.3.3 Speed Trap Switches

Five pressure tape switches, spaced at 2-m intervals, were used to determine the speed of the vehicle before impact. Each tape switch fired a strobe light and sent an electronic timing mark to the data acquisition system as the left-front tire of the test vehicle passed over it. Test vehicle speeds were determined from electronic timing mark data recorded on "EGAA" software. Strobe lights and high-speed film analysis are used only as a backup in the event that vehicle speeds cannot be determined from the electronic data.

4.3.4 Strain Gauges

Post nos. 1 and 2 were instrumented with strain gauges on the back side of the posts approximately 29 mm (1.1 in.) above the ground line. On each post, one gauge was placed on the centerline of the post, while the other gauge was placed approximately 13 mm (½ in.) from the edge. The data from the strain gauges were recorded for 10 seconds, at a rate of 5000 samples/sec.

Weldable strain gauges were used and consisted of gauge type LWK-06-W250B-350. The nominal resistance of the gauges was 350.0 ± 1.4 ohms, with a gauge factor equal to 2.02. The operating temperature limits of the gauges was -195 to +260 degrees Celsius. The strain limits of the gauges were 0.5% in tension or compression (5000 μ). The strain gauges were manufactured by the Micro-Measurements Division of Measurements Group, Inc. of Raleigh, North Carolina. The installation procedure required that the metal surface be clean and free from debris and oxidation. Once the surface

had been prepared, the gauges were spot welded to the test surface.

A Measurements Group Vishay Model 2310 signal conditioning amplifier was used to condition and amplify the low-level signals to high-level outputs for multichannel, simultaneous dynamic recording on "Test Point" software. After each signal was amplified, it was sent to a Keithly Metrabyte DAS-1802HC data acquisition board, and then stored permanently on the portable computer.

5 PERFORMANCE EVALUATION CRITERIA

The safety performance objective of a guardrail to bridge rail transition is to redirect an errant vehicle in a controlled manner without allowing it to snag on the end of the bridge rail, causing excessive deceleration and occupant compartment deformation.

The performance criteria used to evaluate this full-scale vehicle crash test was taken from NCHRP Report 350, *Recommended Procedures for the Safety Performance Evaluation of Highway Features* (2). The safety performance of the bridge rail was evaluated according to three major factors: (1) structural adequacy, (2) occupant risk, and (3) vehicle trajectory after collision. These three evaluation criteria are defined and explained in NCHRP Report 350 (2). The specific evaluation criteria which pertain to this test are presented in Table 1.

After each test, vehicle damage was assessed by the traffic accident scale (TAD) (6) and the vehicle damage index (VDI) (7).

Table 1. Relevant NCHRP 350 Evaluation Criteria

A.	Test article should contain and redirect the vehicle; the vehicle should not penetrate, underide, or override the installation although controlled lateral deflection of the test article is acceptable.
D.	Detached elements, fragments or other debris from the test article should not penetrate or show potential for penetrating the occupant compartment, or present an undue hazard to other traffic, pedestrians, or personnel in a work zone. Deformations of, or intrusions into, the occupant compartment that could cause serious injuries should not be permitted.
F.	The vehicle should remain upright during and after collision although moderate roll, pitching and yawing are acceptable.
K.	After collision it is preferable that the vehicle's trajectory not intrude into adjacent traffic lanes.
L.	The occupant impact velocity in the longitudinal direction should not exceed 12 m/s (39.4 fps) and the occupant ridedown acceleration in the longitudinal direction should not exceed 20 g's.
M.	The exit angle from the test article preferably should be less than 60 percent of test impact angle, measured at time of vehicle loss of contact with test device.

6 TEST RESULTS

6.1 Test NEBT-1 (2,004 kg, 103.2 km/h, 24.9 degrees)

For this test, the 1990 Chevrolet $\frac{3}{4}$ -ton pickup impacted the transition midway between post nos. 1 and 2, as can be seen in Figure 5. The actual impact conditions were 103.2 km/h and 24.9 degrees. The results of the test are summarized in Figure 5, with additional sequential photos presented in Figures 6 and 7.

Upon impact with the approach thrie-beam, the right-front corner of the vehicle began to crush inward. By 14 msec after impact, the right-front corner of the vehicle had reached post no. 1, and by 49 msec, it was at the midpoint between the first post and the bridge end. At 66 msec, the vehicle reached the leading edge of the abutment and the right-front tire began to slide under the rail. At 90 msec after impact, the right-front tire, which had become wedged under the rail, impacted the end of the concrete abutment. This contact caused high deceleration forces and increased the amount of occupant compartment damage which occurred to the vehicle. At 185 msec, the rear bumper contacted the approach rail, and at 201 msec after impact, the vehicle was parallel to the system and traveling at a velocity of 64.4 km/h (40.0 mph). The truck continued to redirect from the system, and exited at 7 degrees and 61.4 km/h (38.2 mph) at 376 msec after impact. The vehicle continued downstream and came to rest approximately 52-m (170-ft) downstream of impact, with the vehicle center of gravity approximately 3 m (10 ft) behind a line parallel with the front face of the guardrail. This final resting position can be seen in Figure 8.

Damage to the system was minimal, as shown in Figure 9. The maximum permanent set deflection in the guardrail of 71 mm (2 $\frac{13}{16}$ in.) occurred at the midspan between the bridge end and the first post. The first post fractured the flowable fill around its base, as a result of rotation during impact. There was

slight cracking of the flowable fill around post no. 2, but no deformation of the post. Damage to the bridge end was very minor, and consisted of tire marks and minor concrete spalling. The tire marks indicated approximately 3 in. of wheel snag on the flat end of the concrete abutment. There were no cracks in the bridge end, and no repair would be necessary for this component of the system.

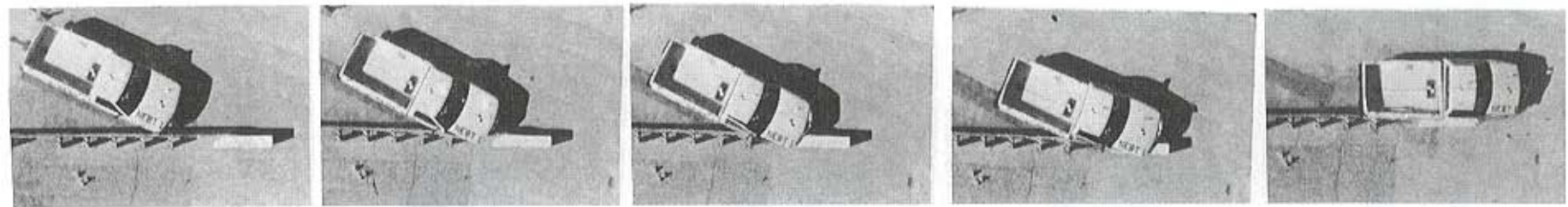
The vehicle damage was considerable, as shown in Figure 10. The entire right-front corner of the vehicle was severely crushed, resulting in deformation of the occupant compartment. The upper control arm was disengaged from the right-front wheel assembly, allowing the wheel to pivot outward and snag on the end of the abutment. Most of the right side of the vehicle was damaged as a result of contact with the transition system.

Deformation measurements in the occupant compartment indicated that the maximum longitudinal and lateral deformations occurred on the right-front corner of the floorboard, which was the closest point to the impacted region. The deformation in the occupant compartment appeared to be more typical of what would be expected during a side-impact type loading, rather than the typical deformation caused by the wheel being forced back into the firewall. The longitudinal deformation was measured to be 165 mm (6½ in.), while the lateral deformation was 121 mm (4¾ in.). The maximum vertical occupant compartment deformation of 244 mm (9.6 in.) occurred in the left-rear corner of the passenger side floorboard. The dash was also deformed, with measurements indicating a 152-mm (6-in.) vertical deformation and 267-mm (10½-in.) deformation in the longitudinal direction.

The occupant risk values for this test were calculated even though NCHRP Report 350 (2) does not require that this test meet any of the criteria. The normalized occupant impact velocities were determined to be 9.8 m/s (32.2 fps) in the longitudinal direction, and the 8.2 m/s (26.9 fps) in the lateral

direction. The highest 10-msec average occupant ridedown decelerations were 7.6 g's (longitudinal) and 10.3 g's (lateral). The results of this occupant risk assessment, as determined from the accelerometer data, are summarized in Figure 5. The accelerometer data analysis is shown in Appendix C.

As a result of the excessive occupant compartment deformation, the performance of Test NEBT-1 on the Nebraska Guardrail to Bridge Rail Transition was determined to be unsuccessful according to the criteria set forth in NCHRP Report 350 (2).



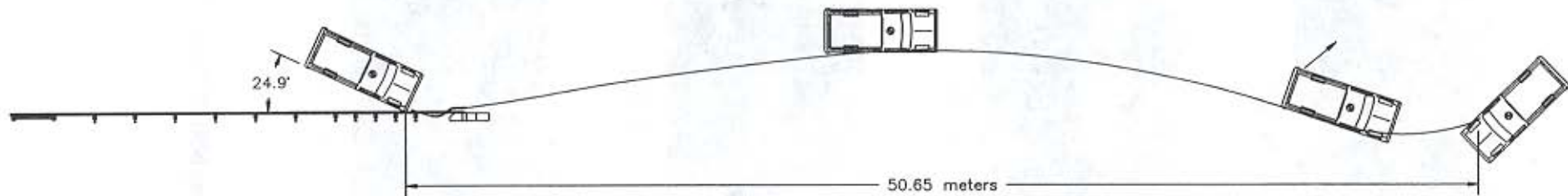
Impact

49 ms

66 ms

109 ms

201 ms



22

Test Number	NEBT-1
NCHRP 350 Test Designation	3-21
Date	10/2/97
Installation	Nebraska Transition
Approach guardrail length	21 m
Steel Posts	
No. 1 & 2	W150x37 (2591 mm long)
No. 3 to 6	W150x22 (2134 mm long)
No. 7 to 11	W150x13.5 (1830 mm long)
Vehicle Model	1990 Chevrolet ¼-ton pickup
Vehicle Weight	
Curb	1868 kg
Test Inertia	2000 kg
Gross Static	2000 kg
Speed	
Impact	103.2 km/h
Exit	61.4 km/h

Angle	
Impact	24.9 deg
Exit	7.0 deg
Change in Velocity	41.8 km/h
Normalized Occupant Impact Velocity	
Longitudinal	9.8 m/s
Lateral	8.2 m/s
Occupant Ridedown Deceleration	
Longitudinal	7.6 G's
Lateral	10.3 G's
Vehicle Damage	
TAD	1-RFQ-5
VDI	01RFES3
Vehicle Rebound Distance	2.9 m @ 24 m
Transition Damage	Minor
Maximum Permanent Set Deflection	71 mm between bridge end and post 1

Conversion Factors: 1 in. = 2.54 cm; 1 lb = 0.454 kg

Figure 5. Summary of Test NEBT-1.



Impact



196 ms



47 ms



290 ms



88 ms



570 ms



112 ms



866 ms

Figure 6. Downstream Sequential Photographs, Test NEBT-1.



Impact



90 ms



36 ms



174 ms



46 ms



194 ms



68 ms



218 ms

Figure 7. Close-up Sequential Photographs, Test NEBT-1.

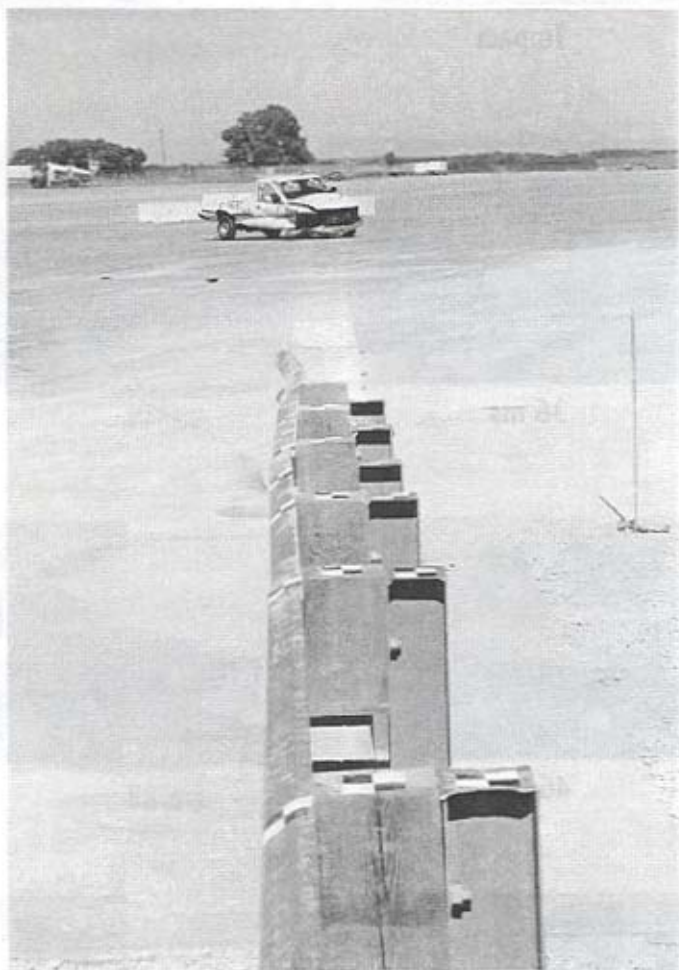


Figure 8. Vehicle Trajectory, Test NEBT-1.

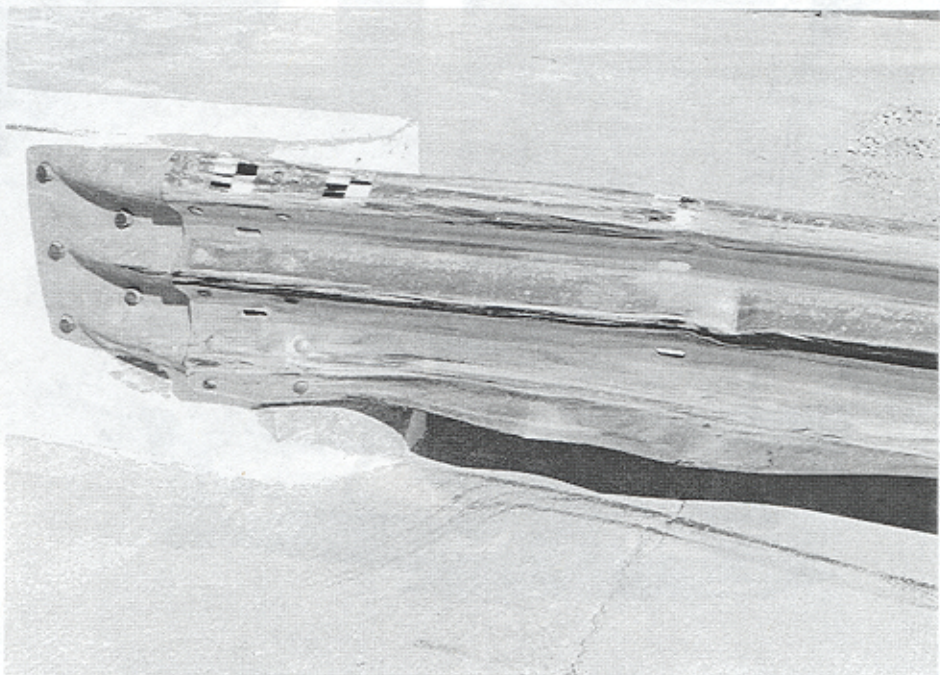
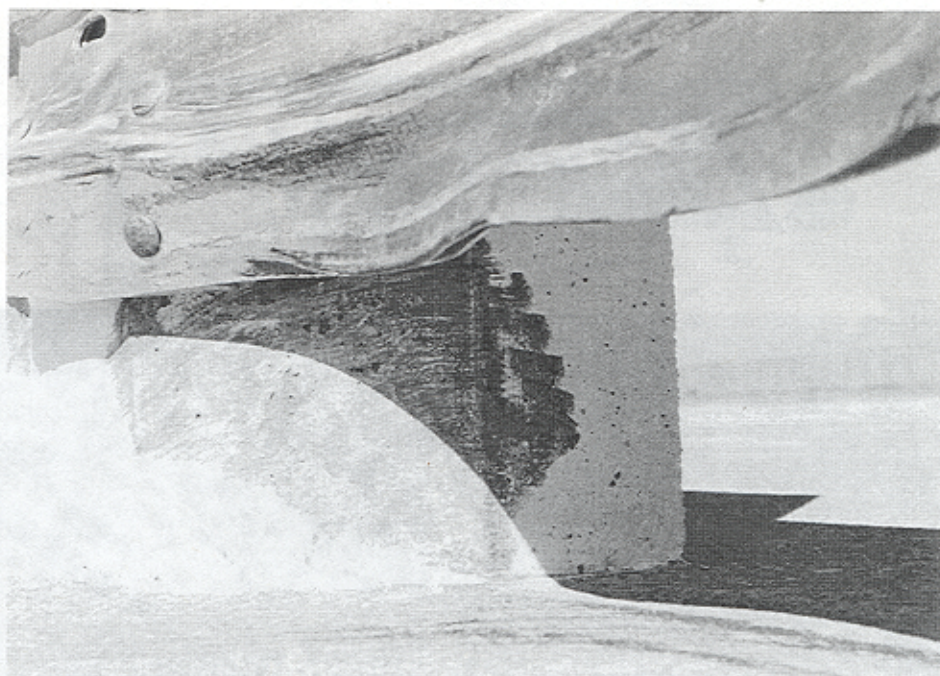


Figure 9. System Damage, Test NEBT-1. (cont'd)
Figure 10. Vehicle Damage, Test NEBT-1.

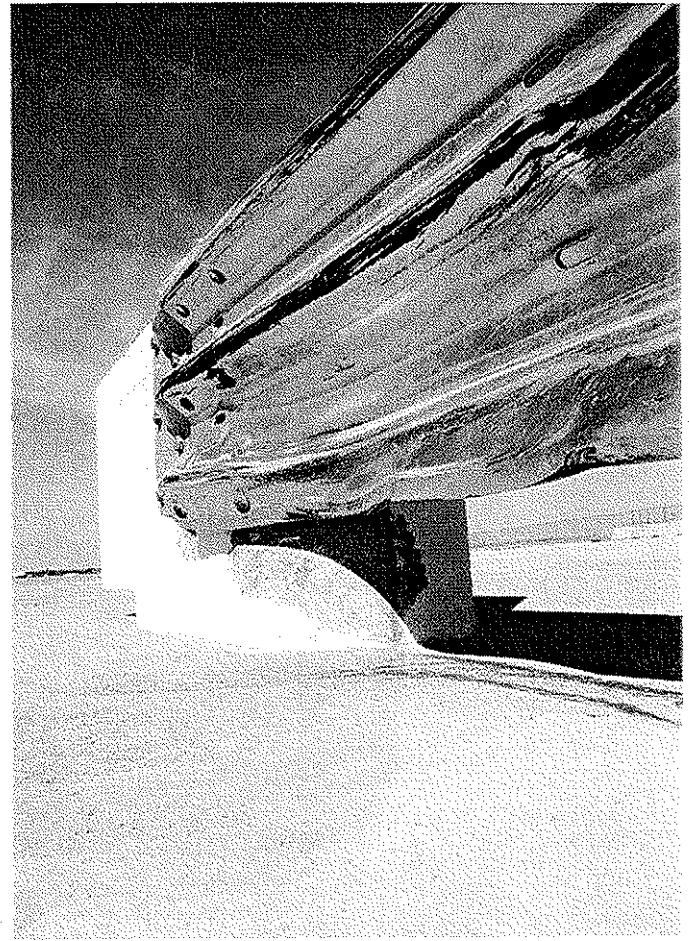


Figure 9. System Damage, Test NEBT-1 (continued).



Figure 10. Vehicle Damage, Test NEBT-1.



Figure 10. Vehicle Damage, Test NEBT-1 (continued).

7 STRAIN GAUGE RESULTS

The data obtained from the strain gauges which were placed on post Nos. 1 and 2 was analyzed and is summarized in Table 2.

Table 2. Strain Gauge Instrumentation Results

Post No.	Location	Maximum Strain (: g)	Maximum Stress (ksi)
2	Flange edge	-503	-15.09
2	Flange midpoint	-468	-14.03
1	Flange edge	-1270	-38.11 (close to yielding depending on exact value of F_y)
1	Flange midpoint	-1225	-36.74 (close to yielding depending on exact value of F_y)

These results indicate that some yielding of the first post likely occurred just below the ground line, indicating that the first post was not over designed. These values are presented for reference, so that they are available for comparison of future tests.

8 DISCUSSION

This transition system behaved remarkably well in its ability to redirect a ¾-ton pickup, as the vehicle was redirected with very little tendency to roll. This is significant because previous tests conducted with pickups on transitions have resulted in high roll angles and rollovers. Vehicle vaulting is also typical in this type of an impact, but did not occur during this test. However, the snagging which occurred on the end of the bridge abutment was critical, as it ultimately resulted in significant deformations of the occupant compartment, and failure of the test. Based on the extent and location of this deformation, it was judged that it would indeed present a risk to occupants involved in an impact.

The amount of occupant compartment deformation which is allowable during a redirection test with a pickup, has become the object of much debate recently, as the structure of a pickup allows for more deformation than was typically found in the older sedan test vehicle. The typical scenario witnessed during a pickup test is that the front wheel is pushed backward into the firewall, causing local deformation of the firewall and floorpan in the longitudinal direction. However, this was not the case in this test, as the deformation appeared to be the result of a lateral force which caused significant deformation to the entire floorboard. This lateral force occurred after the tire extended under the rail, contacted the upstream end of the concrete section, and was forced to move laterally back into the wheel-well region. It is believed that this occurrence was not due to the increased flare rate of the concrete taper but was due to the unique observation of the tire collapsing underneath the rail and contacting the end section.

The original concrete buttress used by NDOR is configured with a tapered concrete end that does not extend to the ground but is elevated 255 mm (10.0 in.) above the roadway. This configuration provides a blunt end at the base of the concrete buttress at the point where the tapered concrete section becomes

flush with the back side of the three beam rail. However, the modified design incorporated a tapered section that continued down to the bridge deck surface. As stated previously, this change was made to improve constructability and reduce the likelihood of wheel snagging on the blunt end below the tapered concrete section. As already mentioned, during the crash test a unique tire failure occurred, causing the wheel to contact on the end of the tapered concrete section. The researchers believe that had the tapered concrete section remained elevated above the roadway surface, the probability of tire contact on the blunt end below the tapered concrete section would be equal to or greater than that found during this crash test.

9 RECOMMENDATIONS

Based on the system performance witnessed during the testing described herein, it is recommended that the Nebraska transition design be modified to include a rubrail. A properly designed rubrail would prevent the snagging which occurred on the end of the bridge rail, and reduce the amount of occupant compartment deformation to an acceptable level.

10 CONCLUSIONS

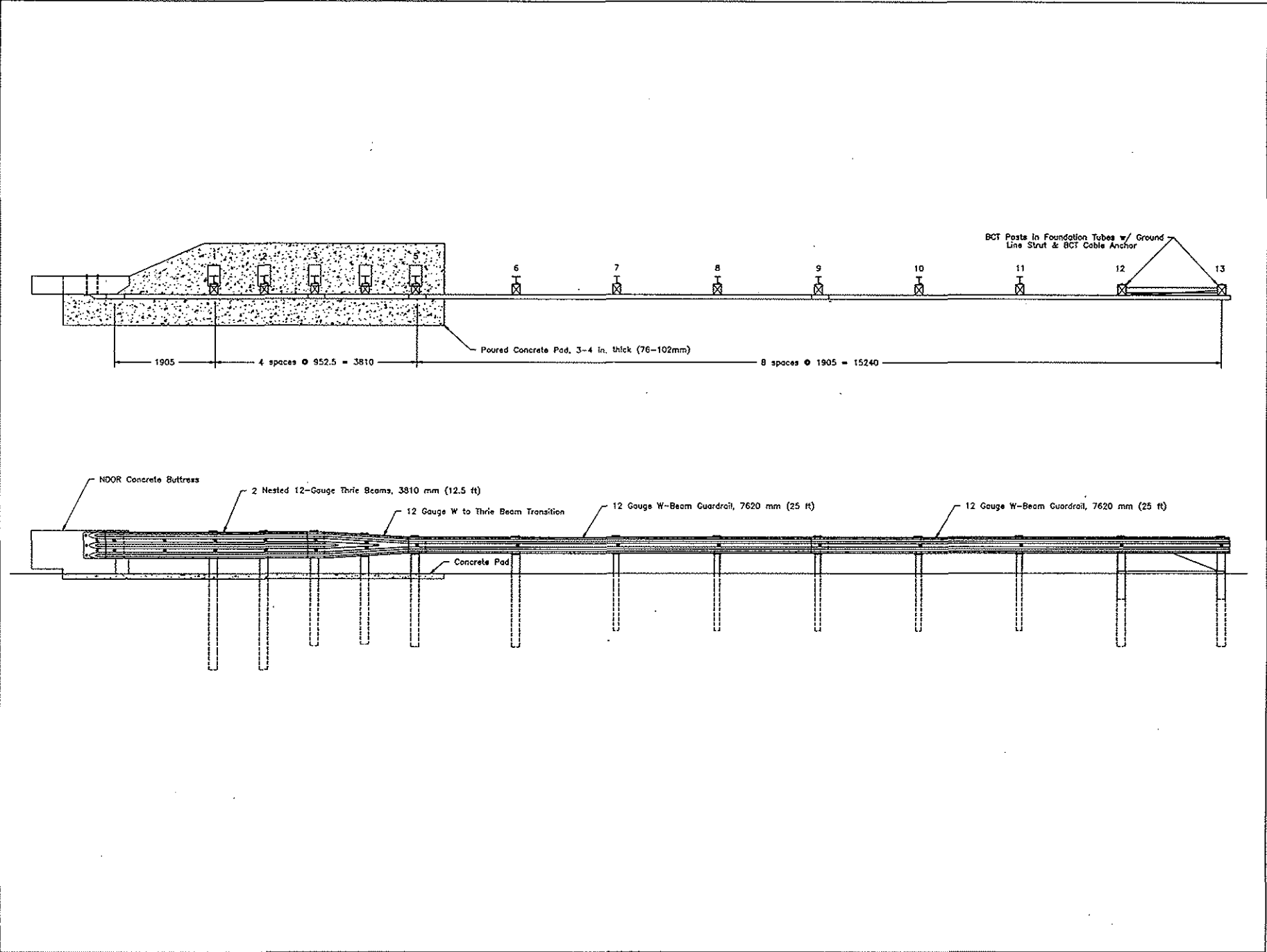
The Nebraska Transition was proven to be capable of redirecting a 3/4-ton pickup in a controlled and predictable manner. However, snagging which occurred on the upstream end of the concrete tapered section resulted in excessive occupant compartment deformations. This led to the conclusion that the system does not pass the Test Level 3 criteria for guardrail to bridge rail transitions which is set forth in NCHRP Report 350 (2).

11 REFERENCES

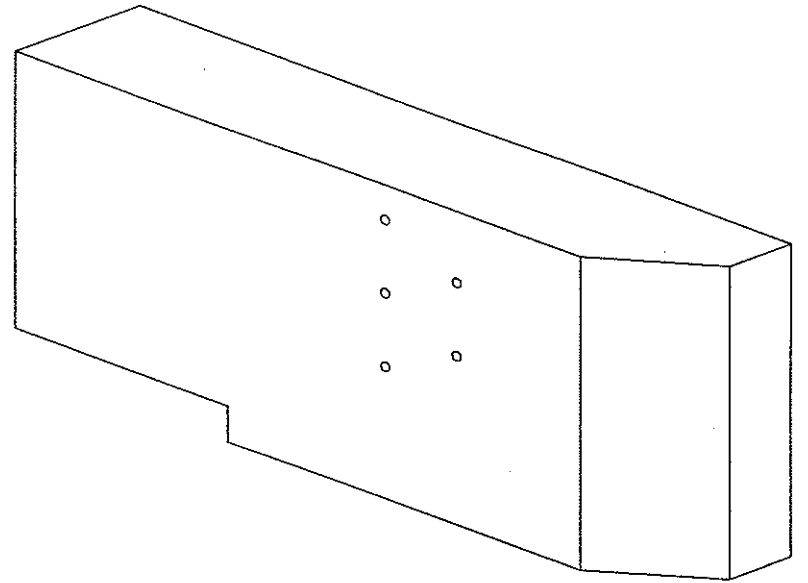
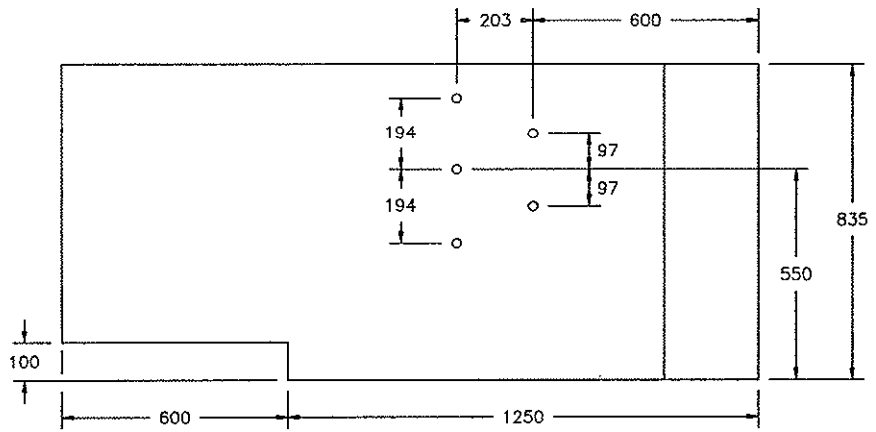
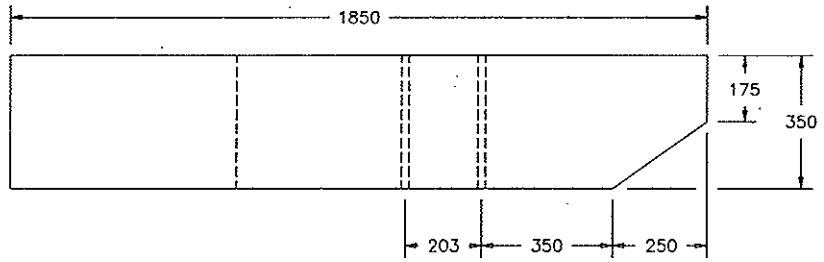
1. *Recommended Procedures for the Safety Performance Evaluation of Highway Appurtenances*, National Cooperative Highway Research Program Report No. 230, Transportation Research Board, Washington, D.C., March 1981.
2. *Recommended Procedures for the Safety Performance Evaluation of Highway Features*, National Cooperative Highway Research Program Report 350, Transportation Research Board, Washington, D.C., 1993.
3. Post, E.R., *Full-Scale Vehicle Crash Tests on Guardrail-Bridgerail Transition Designs with Special Post Spacing*, Transportation Research Report TRP-03-008-87, University of Nebraska-Lincoln, Lincoln, NE, May 1987.
4. Powell, G.H., *BARRIER VII: A Computer Program For Evaluation of Automobile Barrier Systems*, Prepared for: Federal Highway Administration, Report No. FHWA RD-73-51, April 1973.
5. Hinch, J., Yang, T-L, and Owings, R., *Guidance Systems for Vehicle Testings*, ENSCO, Inc., Springfield, VA, 1986.
6. *Vehicle Damage Scale for Traffic Investigators* , Traffic Accident Data Project Technical Bulletin No. 1, National Safety Council, Chicago, IL, 1971.
7. *Collision Deformation Classification, Recommended Practice J224 March 1980* , SAE Handbook Vol. 4, Society of Automotive Engineers, Warrendale, Penn., 1985.

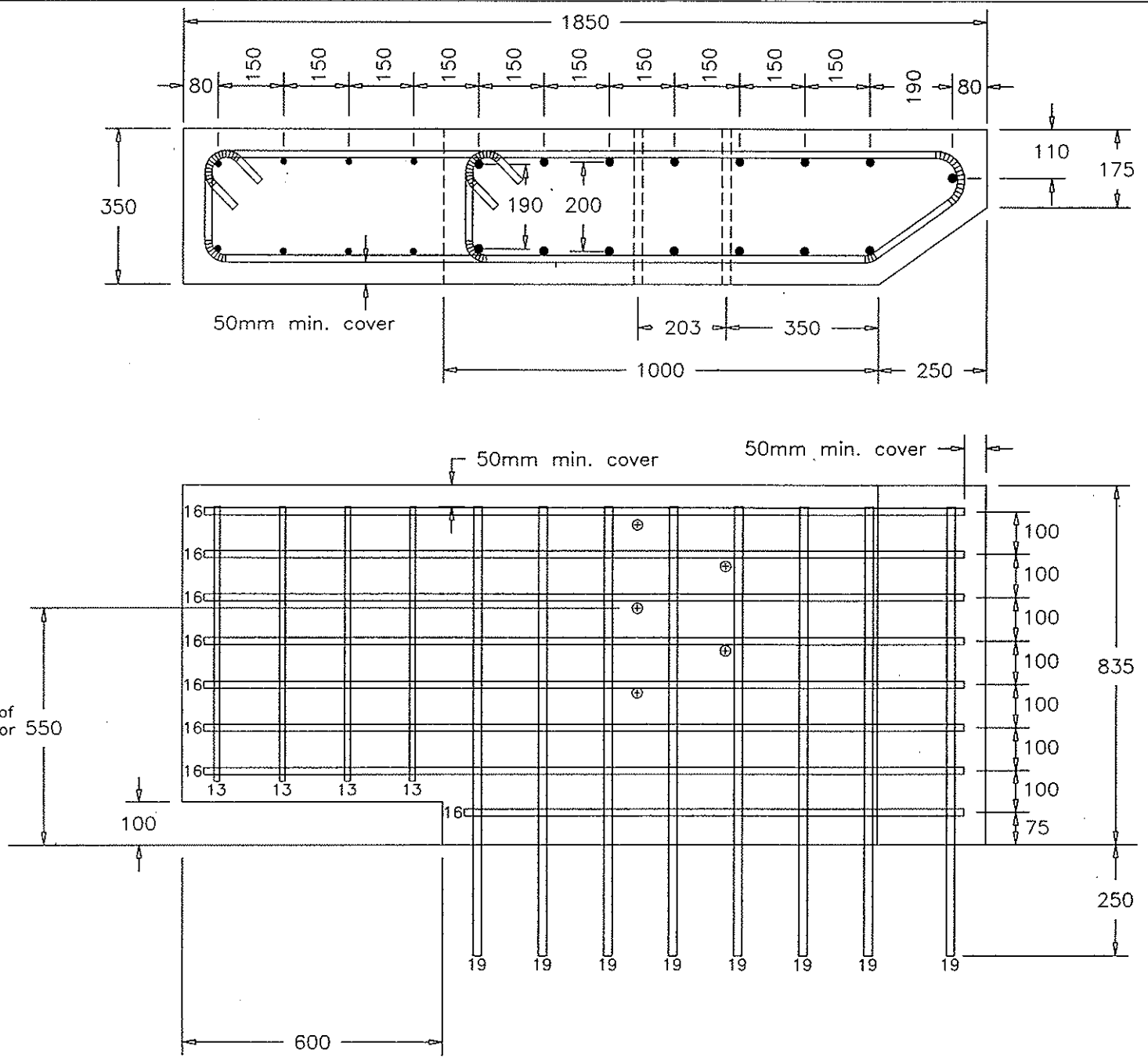
12 APPENDICES

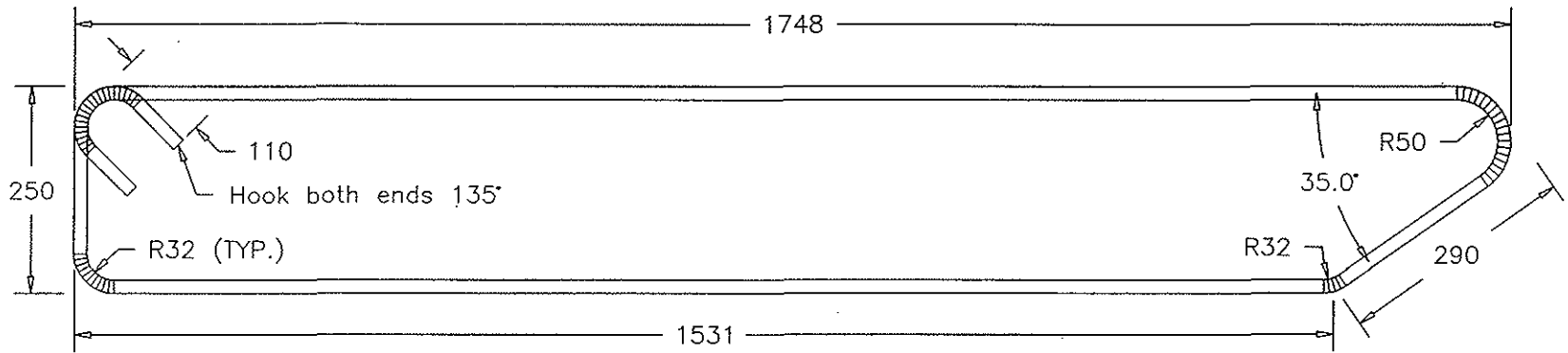
APPENDIX A: Nebraska Transition Design Details



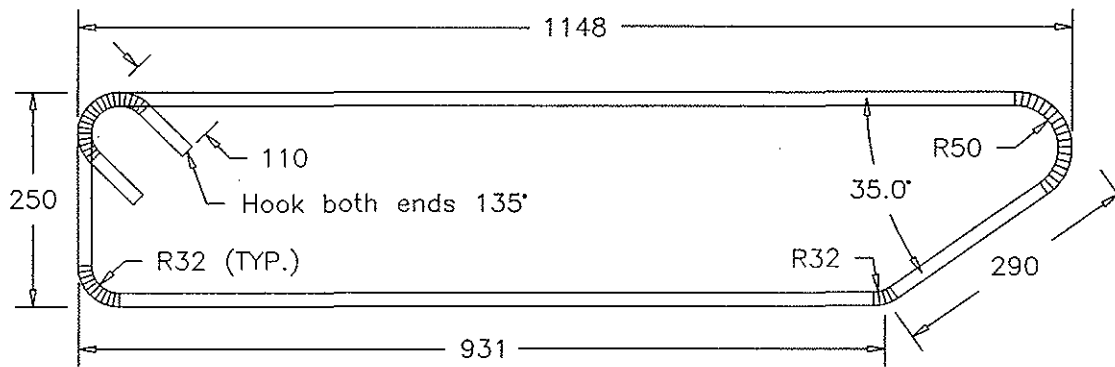
39



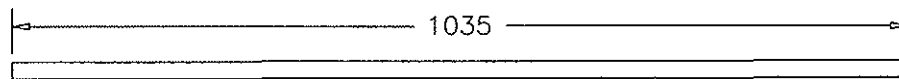




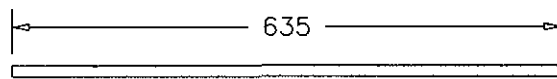
7 each No. 16, Grade 60



1 each No. 16, Grade 60

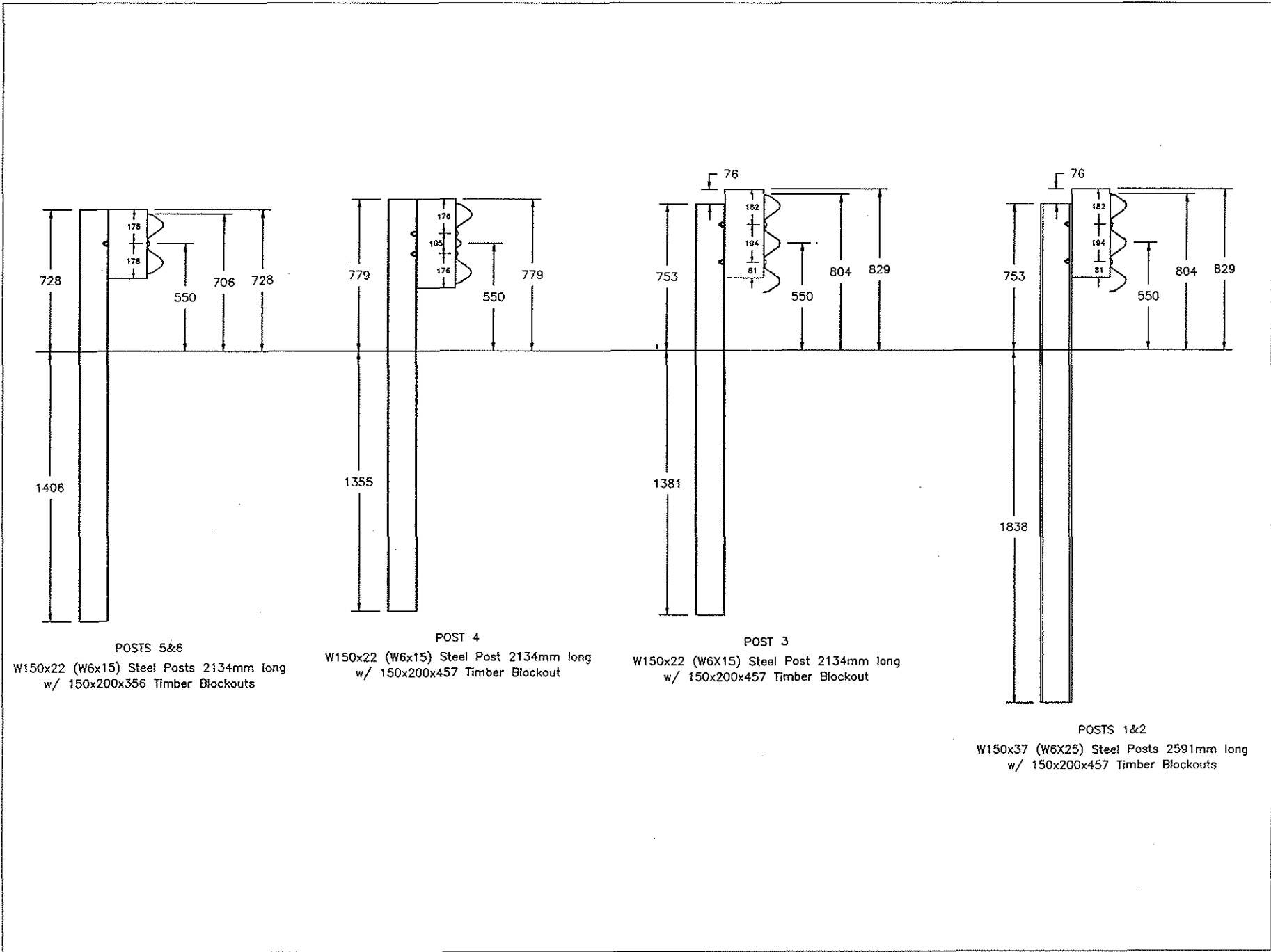


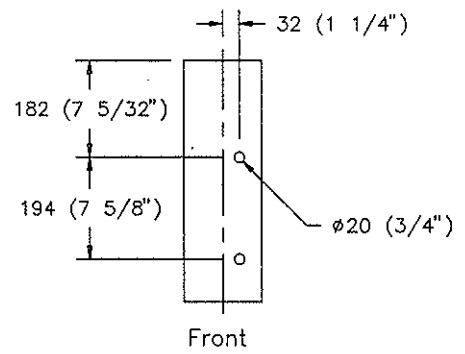
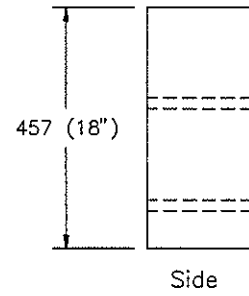
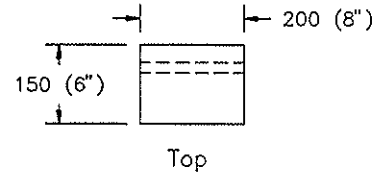
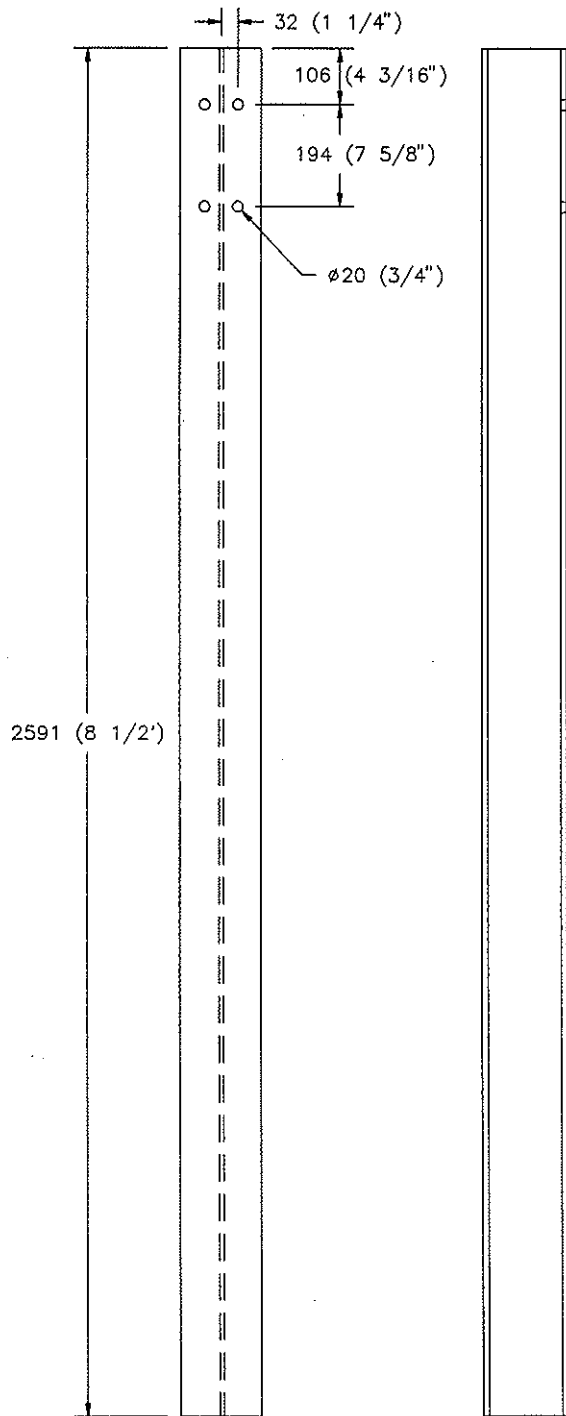
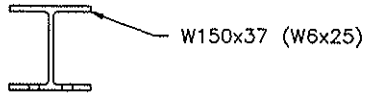
15 each No. 19, Grade 60



8 each No. 13, Grade 60

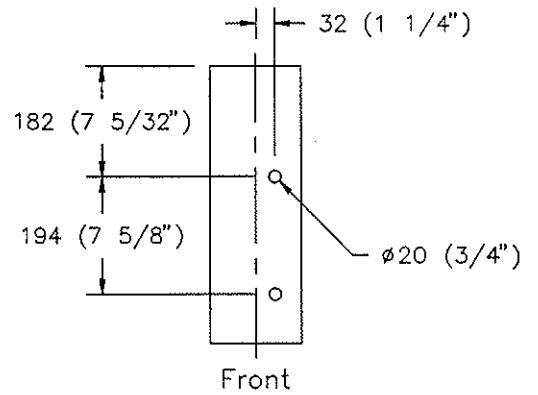
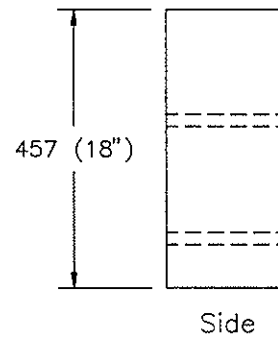
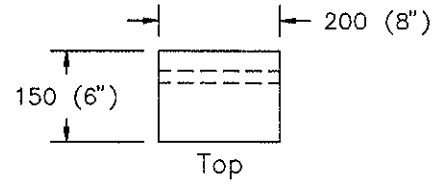
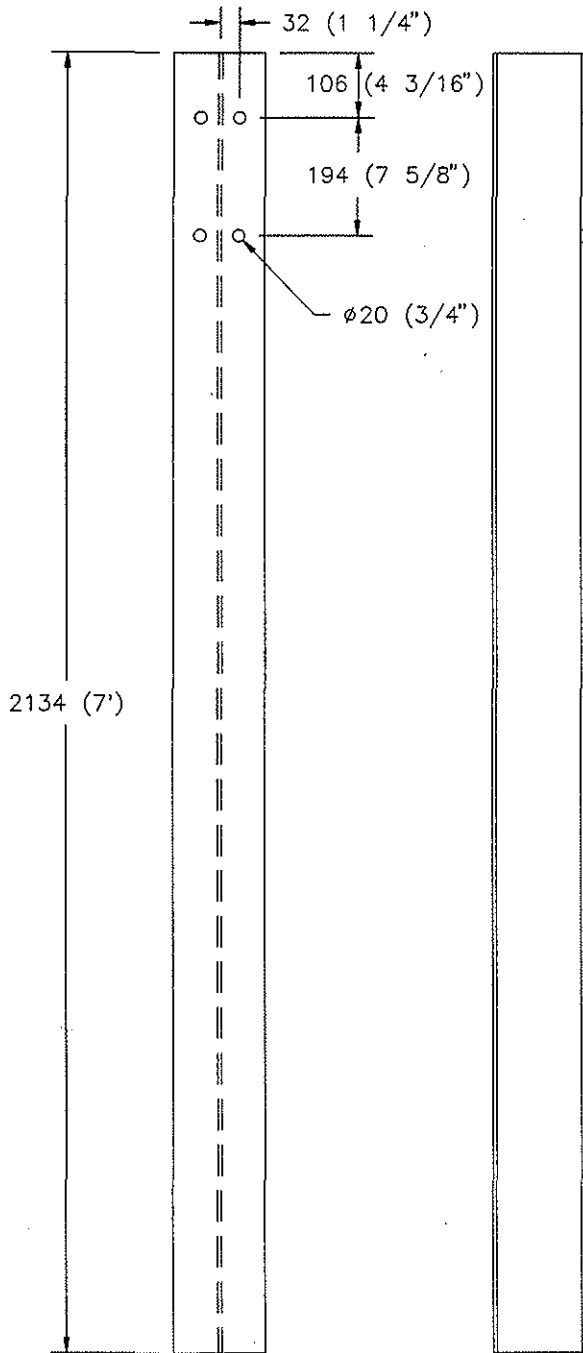
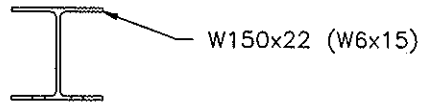
MwRSF		University of Nebraska C.E. Department
NDOR TRANS		
DATE:	8-7-97	
SCALE:	none	
DR'N:	EAK	barsc2





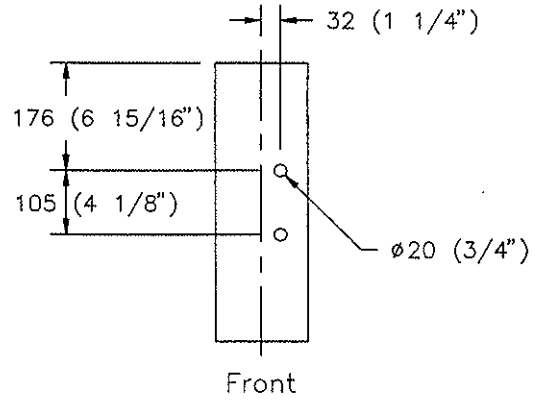
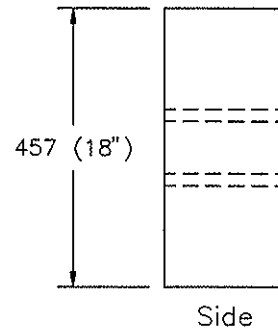
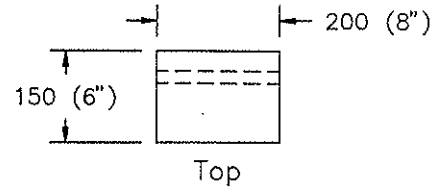
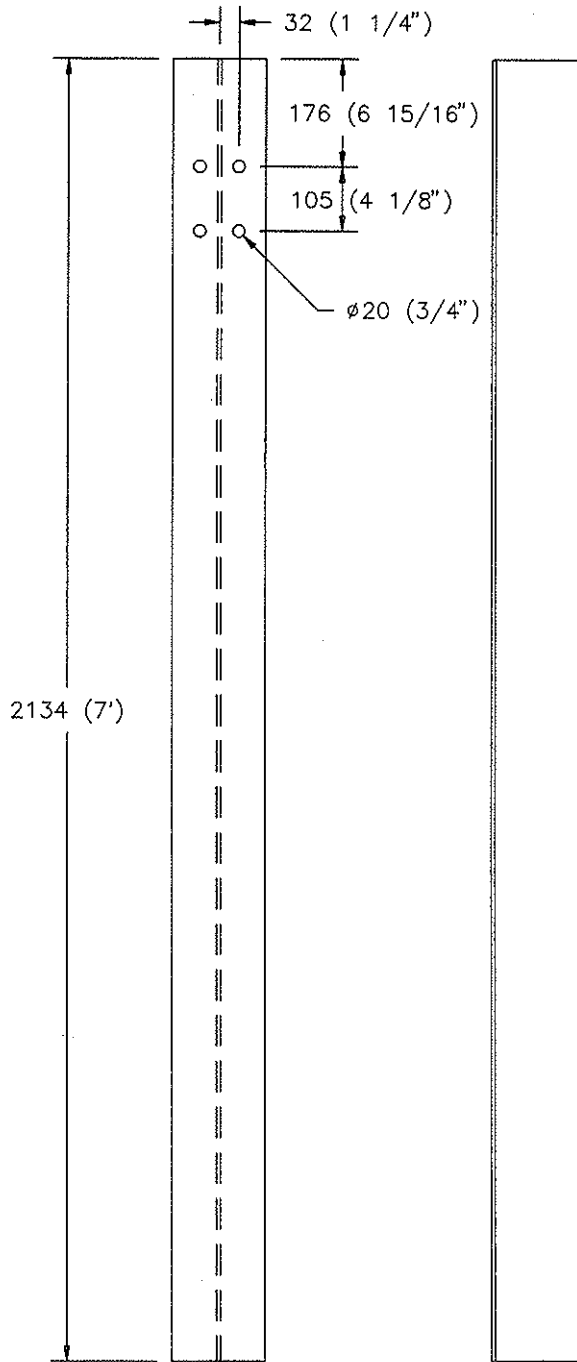
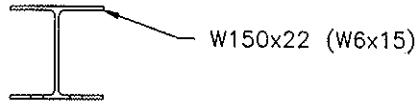
POST NOS. 1 and 2

2 each W150x37 (W6x25) Steel Posts w/ Timber Blockouts



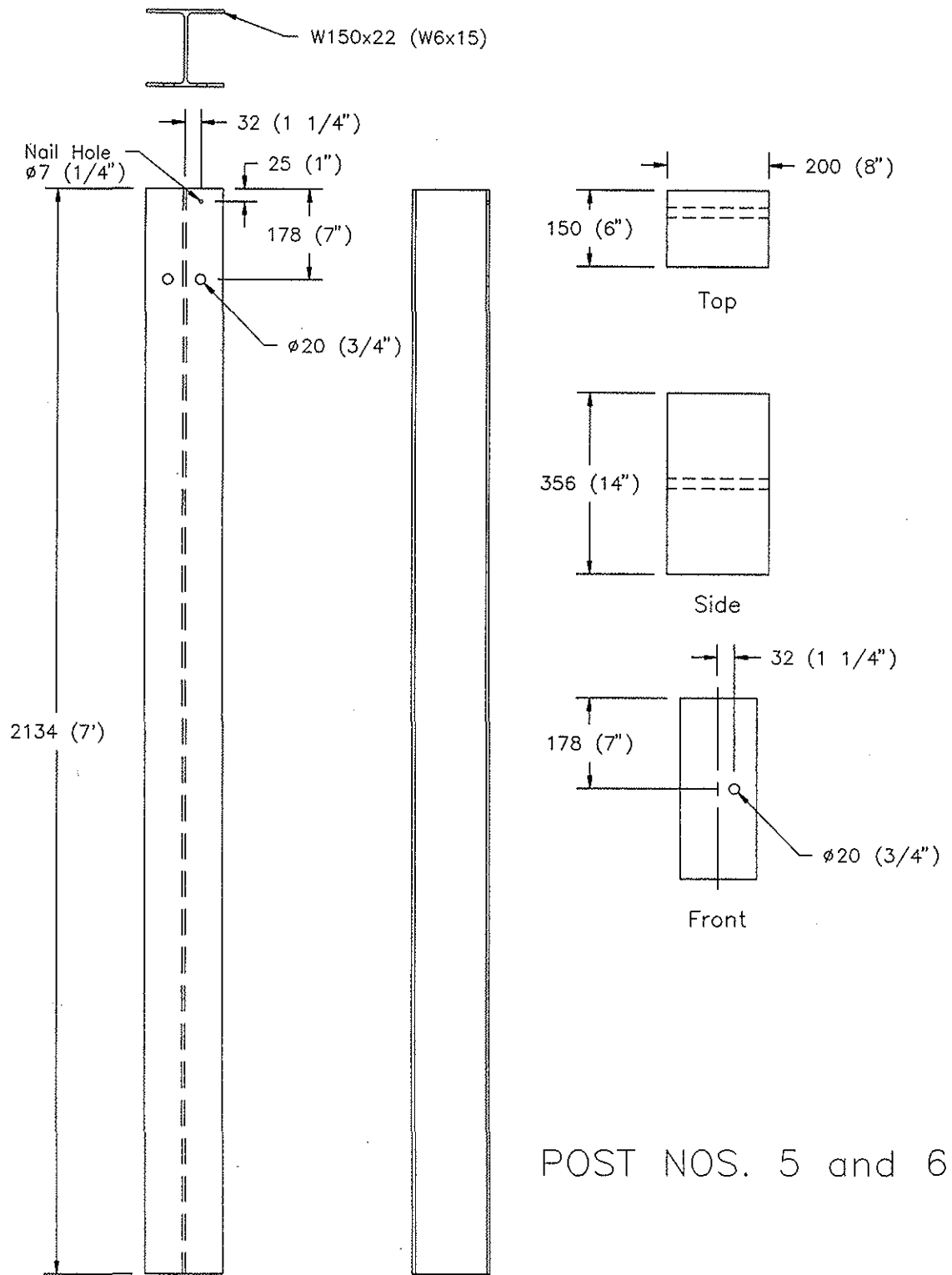
POST NO. 3

1 each W150x22 (W6x15) Steel Posts w/ Timber Blockouts



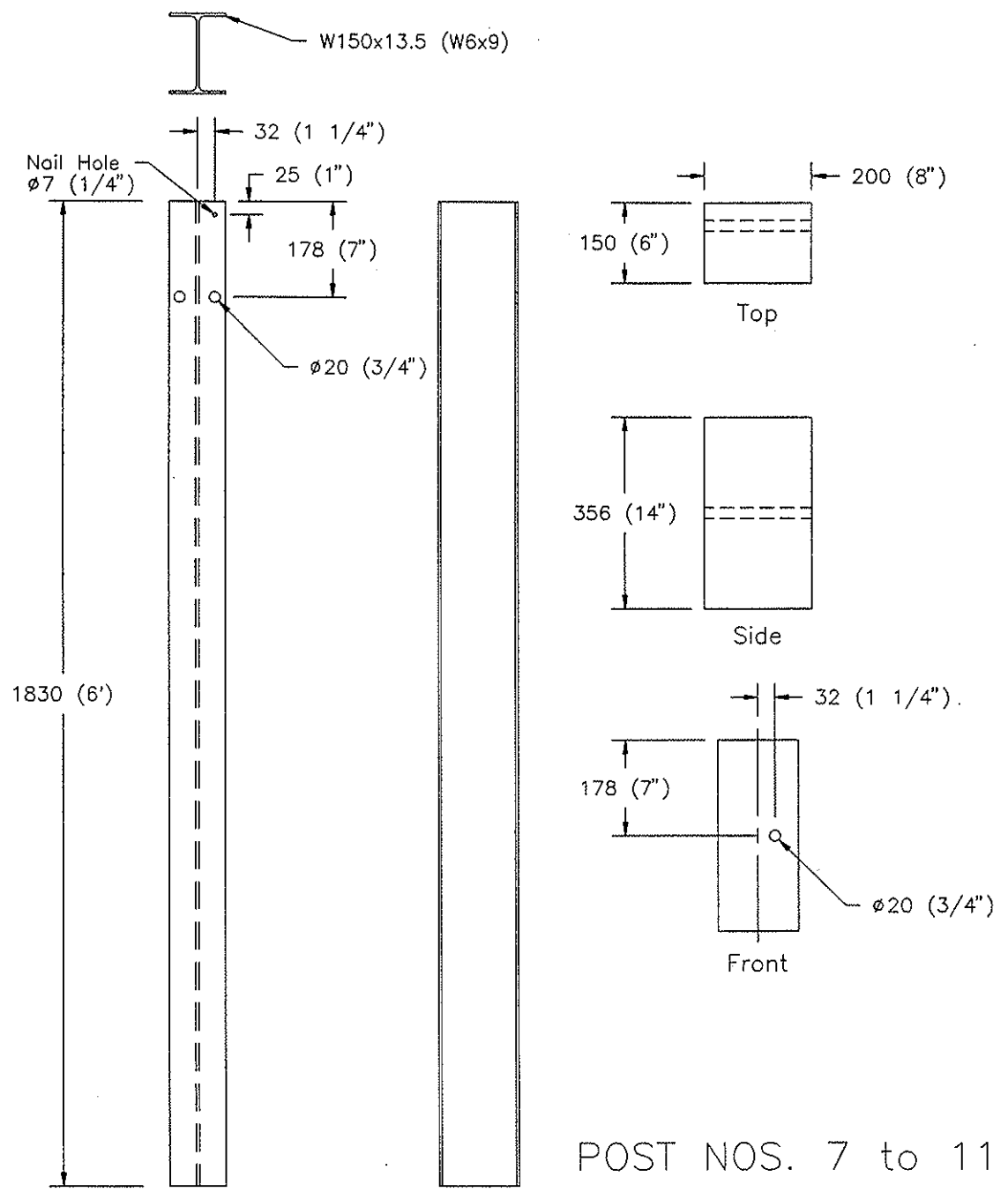
POST NO. 4

1 each W150x22 (W6x15) Steel Posts w/ Timber Blockouts



POST NOS. 5 and 6

2 each W150x22 (W6x15) Steel Posts w/ Timber Blockouts



5 each W150x13.5 (W6x9) Steel Posts w/ Timber Blockouts

SECTION 1003 -- FLOWABLE FILL

1003.01 -- Description

Flowable fill shall be a mixture of cement, fly ash, fine sand, water, and air having a consistency which will flow under a very low head.

1003.02 -- Material Characteristics

1. The approximate quantities of each material per cubic meter of mixed material shall be as follows:

FLOWABLE FILL

Cement (Type I or II)	30 kg
Fly ash	120 kg
Fine sand	1,600 kg
Water (approx.)	250 kg
Air content (approx.)	10%

2. Actual quantities shall be adjusted to provide a yield of one cubic meter with the materials used.

3. Approximate compressive strength should be 6 to 12 kPa.

4. Fine sand shall be a reasonably graded material having not less than 95-percent passing the 4.75 mm sieve and not more than 5-percent passing the 75 μ m sieve.

5. Mixing and handling of the material shall be in accordance with Section 1002 in the 1985 Standard Specifications.

APPENDIX B: BARRIER VII Simulation Input

NEBRASKA'S TRANSITION TO CONCRETE BUTTRESS - BRUN6S2 (2 12-GA. NESTED THRIE/NODE 27)

37	14	13	1	50	13	2	0												
0.0001			0.0001		0.50	300	0	1.0	1										
1	5	5	5	5	5	1													
1		0.0		0.0															
3		75.00		0.0															
5		150.00		0.0															
7		225.00		0.0															
9		300.00		0.0															
11		375.00		0.0															
13		450.00		0.0															
15		525.00		0.0															
17		600.00		0.0															
19		637.50		0.0															
21		675.00		0.0															
25		712.50		0.0															
29		750.00		0.0															
37		825.00		0.0															
1	3	1	1		0.0														
3	5	1	1		0.0														
5	7	1	1		0.0														
7	9	1	1		0.0														
9	11	1	1		0.0														
11	13	1	1		0.0														
13	15	1	1		0.0														
15	17	1	1		0.0														
17	19	1	1		0.0														
19	21	1	1		0.0														
21	25	3	1		0.0														
25	29	3	1		0.0														
29	37	7	1		0.0														
1	37		0.35																
37	36	35	34	33	32	31	30	29	28										
27	26	25	24	23	22	21	20	19	18										
17	16	15	14	13	12	11	10	9	8										
7	6	5	4	3	2	1													
100	6																		
1	2.30		1.99		37.50		30000.0		6.92		99.5		68.5		0.10				
2	2.475		2.125		18.75		30000.0		7.405		106.25		73.75		0.10				
3	2.84		2.40		18.75		30000.0		8.375		120.0		84.0		0.10				
4	3.205		2.68		18.75		30000.0		9.35		134.0		94.0		0.10				
5	3.575		2.96		18.75		30000.0		10.325		148.0		104.25		0.10				
6	7.52		6.20		9.375		30000.0		21.62		310.0		219.0		0.10				
300	7																		
1	21.65		0.0		1000.0		1000.0		250.0		1000.0		1000.0		0.10				
2	200.0	200.0		2.0		2.0		2.46		54.0		96.6		255.57		0.10			
3	6.0	15.0		16.0		16.0		8.00		8.00		97.5		256.5		495.78		0.10	
4	15.0	30.0		16.0		16.0		8.00		8.00		105.0		256.5		580.87		0.10	
5	15.0	30.0		16.0		16.0		8.00		8.00		105.0		256.5		539.52		0.10	
6	15.0	30.0		16.0		16.0		8.00		8.00		212.5		462.24		984.21		0.10	
7	20.0	55.0		16.0		16.0		8.00		8.00		212.5		462.24		984.21		0.10	
7	21.65		0.0		2000.0		2000.0		500.0		2500.0		2500.0		0.10				
400.0	400.0			1.0		1.0													
1	1	2	16	1	101		0.0		0.0		0.0		0.0		0.0				
17	17	18		1	102		0.0		0.0		0.0		0.0		0.0				
18	18	19		1	103		0.0		0.0		0.0		0.0		0.0				
19	19	20		1	104		0.0		0.0		0.0		0.0		0.0				
20	20	21		1	105		0.0		0.0		0.0		0.0		0.0				
21	21	22		1	106		0.0		0.0		0.0		0.0		0.0				
37	1		38	2	301		0.0		0.0		0.0		0.0		0.0		0.0	0.0	0.0
39	5		43	2	302		0.0		0.0		0.0		0.0		0.0		0.0	0.0	0.0
44	15		45	2	303		0.0		0.0		0.0		0.0		0.0		0.0	0.0	0.0
46	19				304		0.0		0.0		0.0		0.0		0.0		0.0	0.0	0.0
47	21				305		0.0		0.0		0.0		0.0		0.0		0.0	0.0	0.0
48	25		49	4	306		0.0		0.0		0.0		0.0		0.0		0.0	0.0	0.0
50	37				307		0.0		0.0		0.0		0.0		0.0		0.0	0.0	0.0
4400.0	40000.0		20	6	4	0	1												
1	0.055		0.12		6.00		17.0												
2	0.057		0.15		7.00		18.0												
3	0.062		0.18		10.00		12.0												
4	0.110		0.35		12.00		6.0												
5	0.35		0.45		6.00		5.0												
6	1.45		1.50		15.00		1.0												
1	100.75		15.875	1		12.0	1	0	0	0									
2	100.75		27.875	1		12.0	1	0	0	0									
3	100.75		39.875	2		12.0	1	0	0	0									
4	88.75		39.875	2		12.0	1	0	0	0									
5	76.75		39.875	2		12.0	1	0	0	0									
6	64.75		39.875	2		12.0	1	0	0	0									
7	52.75		39.875	2		12.0	1	0	0	0									
8	40.75		39.875	2		12.0	1	0	0	0									
9	28.75		39.875	2		12.0	1	0	0	0									

10	16.75	39.875	2	12.0	1	0	0	0
11	-13.25	39.875	3	12.0	1	0	0	0
12	-33.25	39.875	3	12.0	1	0	0	0
13	-53.25	39.875	3	12.0	1	0	0	0
14	-73.25	39.875	3	12.0	1	0	0	0
15	-93.25	39.875	3	12.0	1	0	0	0
16	-113.25	39.875	4	12.0	1	0	0	0
17	-113.25	-39.875	4	12.0	0	0	0	0
18	100.75	-39.875	1	12.0	0	0	0	0
19	69.25	37.75	5	1.0	1	0	0	0
20	-62.75	37.75	6	1.0	1	0	0	0
1	69.25	32.75		0.0	608.			
2	69.25	-32.75		0.0	608.			
3	-62.75	32.75		0.0	492.			
4	-62.75	-32.75		0.0	492.			
1	0.0	0.0						
3	731.25	0.0	25.0	62.14		0.0	0.0	1.0

APPENDIX C: Accelerometer Data Analysis - Test NEBT-1

Figure C-1. Lateral Deceleration, Test NEBT-1.

Figure C-2. Lateral Change in Velocity, Test NEBT-1.

Figure C-3. Longitudinal Deceleration, Test NEBT-1.

Figure C-4. Relative Longitudinal Change in Velocity, Test NEBT-1.

W6: LATERAL DECELERATION - TEST NEBT-1 (EDR-4)

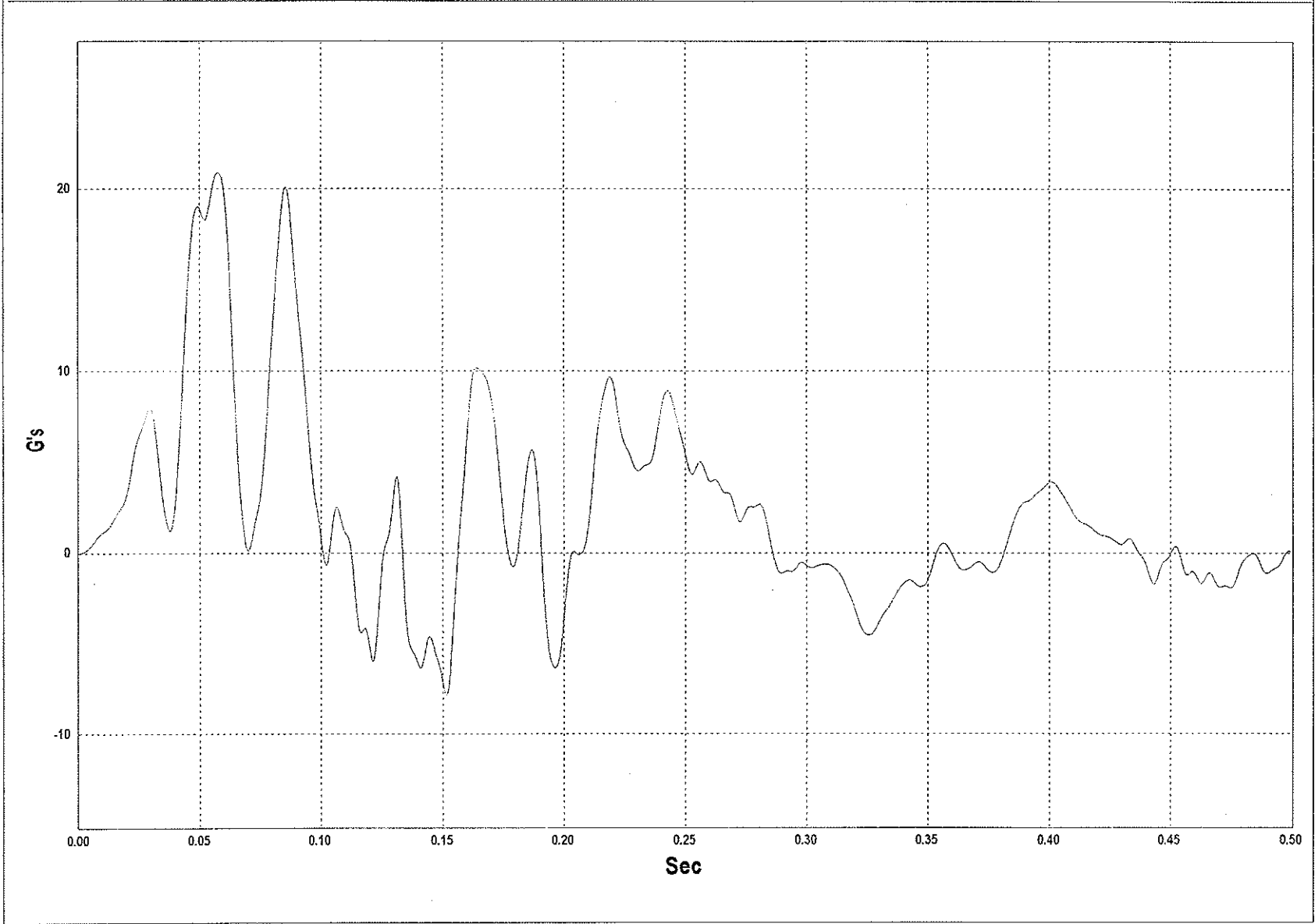


Figure C-1. Lateral Deceleration, Test NEBT-1.

W7: LATERAL OCCUPANT IMPACT VELOCITY - TEST NEBT-1 (EDR-4)

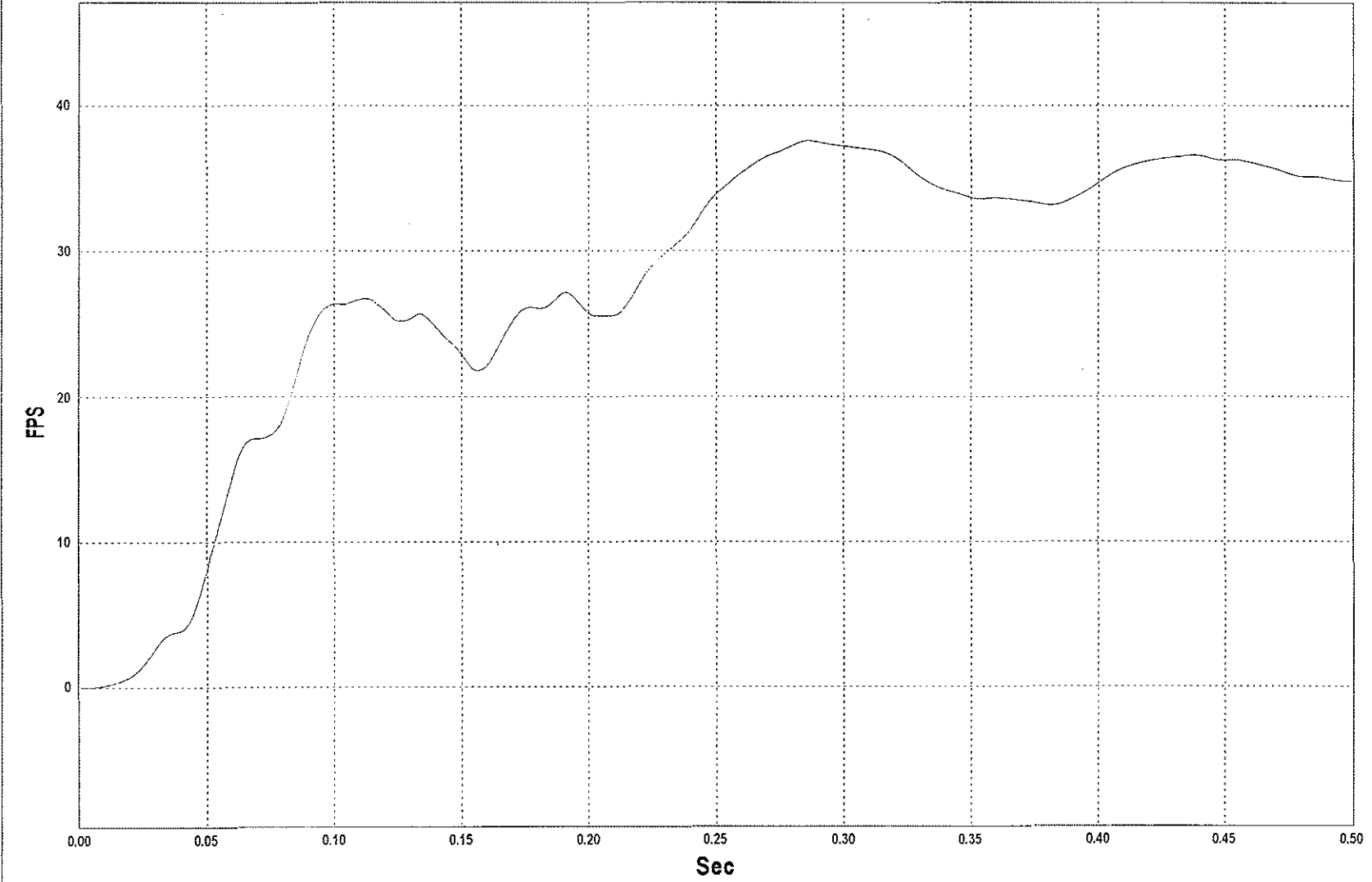


Figure C-2. Lateral Change in Velocity, Test NEBT-1.

W6: LONGITUDINAL DECELERATION - TEST NEBT-1 (EDR-4)

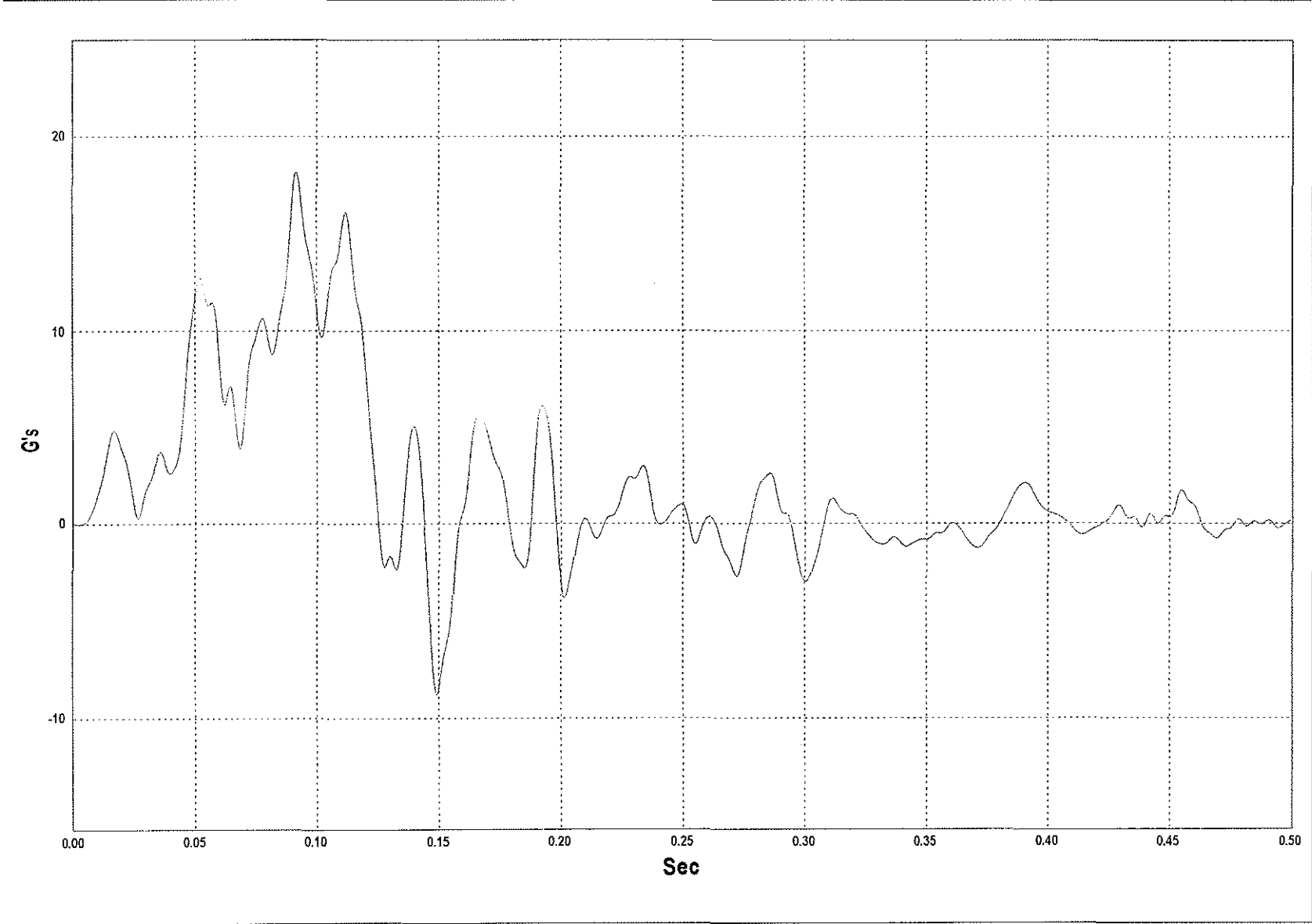


Figure C-3. Longitudinal Deceleration, Test NEBT-1.

W7: LONGITUDINAL OCCUPANT IMPACT VELOCITY - TEST NEBT-1 (EDR-4)

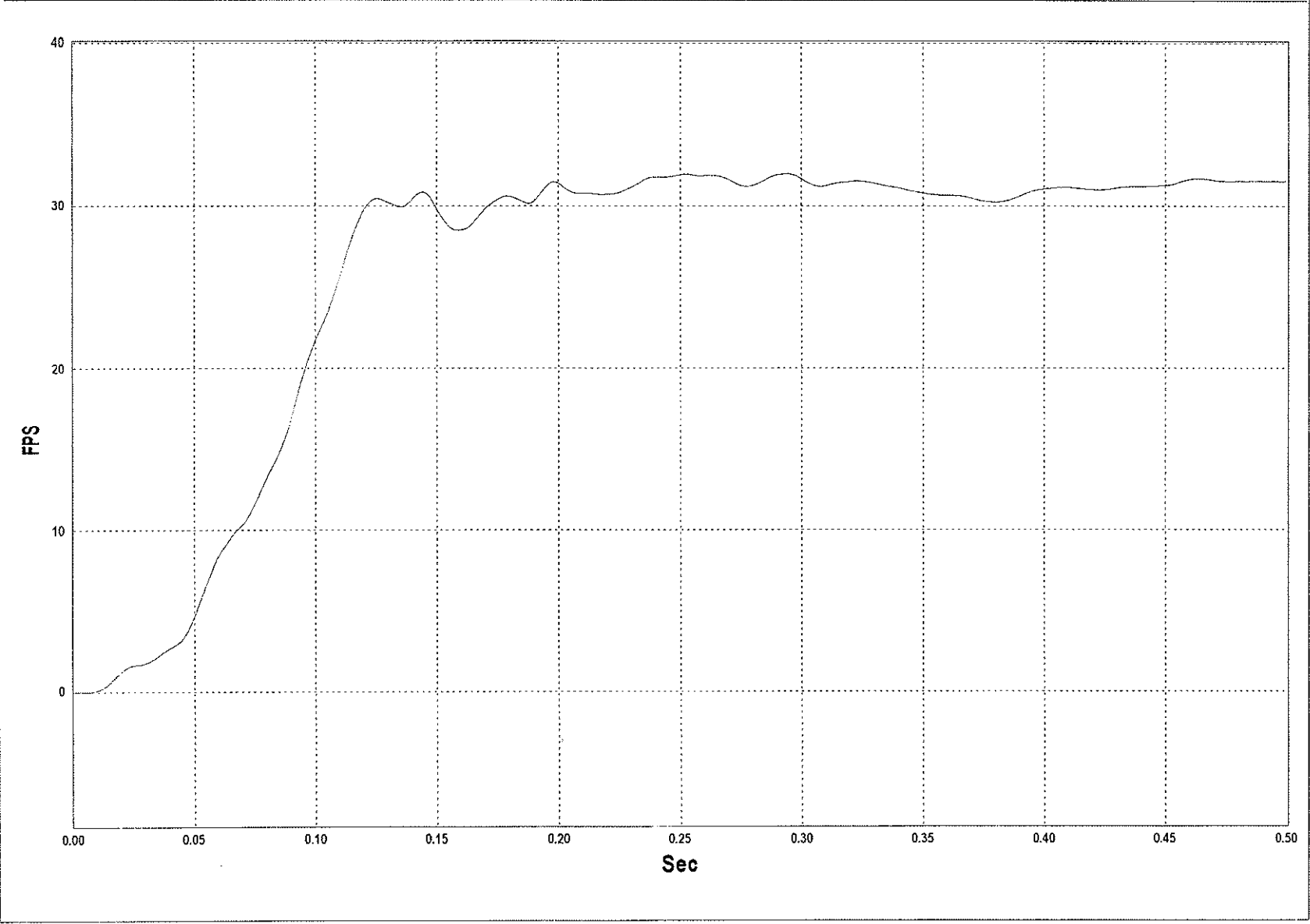


Figure C-4. Relative Longitudinal Change in Velocity, Test NEBT-1.